

Systematic approach to exclusive $B \rightarrow V\ell^+\ell^-, V\gamma$ decays

M. BENEKE, TH. FELDMANN and D. SEIDEL

Institut für Theoretische Physik E, RWTH Aachen, 52056 Aachen, Germany

Abstract

We show – by explicit computation of first-order corrections – that the QCD factorization approach previously applied to hadronic two-body decays and to form factor ratios also allows us to compute non-factorizable corrections to exclusive, radiative B meson decays in the heavy quark mass limit. This removes a major part of the theoretical uncertainty in the region of small invariant mass of the photon. We discuss in particular the decays $B \rightarrow K^*\gamma$ and $B \rightarrow K^*\ell^+\ell^-$ and complete the calculation of corrections to the forward-backward asymmetry zero. The new correction shifts the asymmetry zero by 30%, but the result confirms our previous conclusion that the asymmetry zero provides a clean phenomenological determination of the Wilson coefficient C_9 .

(submitted to Nucl. Phys. B)

1 Introduction

Radiative B meson decays are interesting because they proceed entirely through loop effects. The chiral nature of weak interactions implies additional suppression factors thus enhancing the sensitivity of radiative decays to virtual effects in theories beyond the standard theory of flavour violation, if these new effects violate chirality. The observation of $b \rightarrow s\gamma$ transitions [1] with a branching ratio of about 10^{-4} (in agreement with the standard theory) has since provided significant constraints on extensions of the standard model. The semi-leptonic decay $b \rightarrow s\ell^+\ell^-$ is expected to occur with a branching fraction of a few times 10^{-6} and will probably be first observed in the near future.

Radiative flavour-changing neutral current transitions can be measured inclusively over the hadronic final state (containing strangeness in the particular case considered here) or exclusively by tagging a particular light hadron, typically a kaon. The inclusive measurement is experimentally more difficult but theoretically simpler to interpret, since the decay rate is well and systematically approximated by the decay of a free b quark into light quarks and gluons. In the long run, however, the easier detection of exclusive transitions requires the development of a systematic theoretical framework for these modes as well.

The theoretical difficulty with exclusive decay modes is usually phrased as the need to know the hadronic form factors for the $B \rightarrow K^{(*)}$ transition, but this is only one aspect of the problem. Even if the form factors were known with infinite precision, the present treatment of exclusive, radiative decays would be incomplete, because there exist “non-factorizable” strong interaction effects that do not correspond to form factors. They arise from electromagnetic corrections to the matrix elements of purely hadronic operators in the weak effective Hamiltonian. We compute these non-factorizable corrections in this paper and demonstrate that exclusive, radiative decays can be treated in a similarly systematic manner as their inclusive counterparts. As a result we obtain the branching fractions for $B \rightarrow K^*\gamma$ and $B \rightarrow K^*\ell^+\ell^-$ for small invariant mass of the lepton pair to next-to-leading logarithmic (NLL) order in renormalization-group-improved perturbation theory. (In another commonly used terminology that takes into account the $1/\alpha_s$ enhancement of the semileptonic operator \mathcal{O}_9 the result would be referred to as next-to-next-to-leading logarithmic. However, in order not to have to distinguish in terminology the photonic and semileptonic decay, we shall refer to both as NLL when actually NNLL is meant for the semileptonic decay. Furthermore, since some of the 3-loop anomalous dimensions required for the semileptonic decay are still not computed, the accuracy is not strictly NNLL.)

Our method draws heavily on methods developed recently for other exclusive B decays. In [2, 3] power counting in the heavy quark mass limit and standard factorization arguments for hard strong interaction processes have been used to demonstrate that decay amplitudes for hadronic two-body decays of B mesons can be systematically computed in terms of form factors, light-cone distribution amplitudes and perturbative hard scattering kernels. A similar reasoning has been applied by two of us [4] to hadronic form factors for B decays into light mesons in the kinematic region of large recoil of the light meson. We also noted that a combination of the work on non-leptonic decays and on form factors could be used to compute non-factorizable corrections to radiative

decay amplitudes. Furthermore, the ten different form factors that exclusive decays may depend on can be reduced to only three [5]. More precisely (but still schematically), the amplitude can be represented as

$$\langle \ell^+ \ell^- \bar{K}_a^* | H_{\text{eff}} | \bar{B} \rangle = C_a \xi_a + \Phi_B \otimes T_a \otimes \Phi_{K^*}, \quad (1)$$

where $a = \perp, \parallel$ refers to a transversely and longitudinally polarized K^* , respectively. (An analogous result applies to the decay into a pseudoscalar meson, but we specify our notation to a vector meson for simplicity.) In this equation ξ_a represent universal heavy-to-light form factors [4, 5] and Φ light-cone-distribution amplitudes. The factors C_a and T_a are calculable in renormalization-group improved perturbation theory. Previous treatments of exclusive radiative decays correspond to evaluating (1) to leading logarithmic accuracy (up to a weak annihilation contribution as we discuss below). The main result of this paper is to show that systematic improvement is possible and to extend the accuracy to the next order. In Section 2 we present the result of the calculation. In Section 3 we first discuss the inputs to our numerical result, such as Wilson coefficients and meson parameters. We then analyse the stability of the result with respect to the input parameters and a variation of the renormalization scale. The phenomenological analysis is given in the subsequent two sections. Section 4 is devoted to $B \rightarrow K^* \gamma$; Section 5 to $B \rightarrow K^* \ell^+ \ell^-$. We focus in particular on corrections to the forward-backward asymmetry, which is independent on the form factors ξ_a to first approximation. In the final Section 6 we discuss power corrections related to photon structure on a qualitative level and summarize our conclusions.

2 Non-factorizable corrections

We generally neglect doubly Cabibbo-suppressed contributions to the decay amplitude. The weak effective Hamiltonian is then given by

$$H_{\text{eff}} = -\frac{G_F}{\sqrt{2}} V_{ts}^* V_{tb} \sum_{i=1}^{10} C_i(\mu) \mathcal{O}_i(\mu), \quad (2)$$

and we use the operator basis introduced in [6] for the operators \mathcal{O}_i , $i = 1, \dots, 6$. (More precisely, due to the normalization of (2), $\mathcal{O}_i = 4P_i$ with P_i defined in [6].) We define

$$\mathcal{O}_7 = -\frac{g_{\text{em}} \hat{m}_b}{8\pi^2} \bar{s} \sigma^{\mu\nu} (1 + \gamma_5) b F_{\mu\nu}, \quad \mathcal{O}_8 = -\frac{g_s \hat{m}_b}{8\pi^2} \bar{s}_i \sigma^{\mu\nu} (1 + \gamma_5) T_{ij}^A b_j G_{\mu\nu}^A, \quad (3)$$

$$\mathcal{O}_{9,10} = \frac{\alpha_{\text{em}}}{2\pi} (\bar{\ell} \ell)_{V,A} (\bar{s} b)_{V-A}, \quad (4)$$

where $\alpha_{\text{em}} = g_{\text{em}}^2/4\pi$ is the fine-structure constant and $\hat{m}_b(\mu)$ the b quark mass in the $\overline{\text{MS}}$ scheme. We shall later trade the $\overline{\text{MS}}$ mass for the pole mass m_b and the PS mass $m_{b,\text{PS}}$. To next-to-leading order the pole and $\overline{\text{MS}}$ masses are related by

$$\hat{m}_b(\mu) = m_b \left(1 + \frac{\alpha_s C_F}{4\pi} \left[3 \ln \frac{m_b^2}{\mu^2} - 4 \right] + O(\alpha_s^2) \right), \quad (5)$$

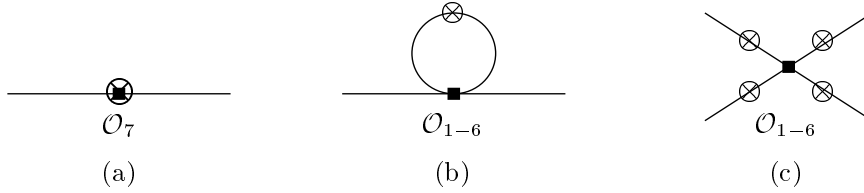


Figure 1: Leading contributions to $\langle \gamma^* \bar{K}^* | H_{\text{eff}} | \bar{B} \rangle$. The circled cross marks the possible insertions of the virtual photon line.

with $\alpha_s \equiv \alpha_s(\mu)$. The sign convention for $\mathcal{O}_{7,8}$ corresponds to a negative $C_{7,8}$ and $+ig_s T^A$, $+ig_{\text{em}} e_f$ for the ordinary quark–gauge-boson vertex ($e_f = -1$ for the lepton fields). We will present our result in terms of “barred” coefficients \bar{C}_i (for $i = 1, \dots, 6$), defined as certain linear combinations of the C_i as described in Appendix A. The linear combinations are chosen such that the \bar{C}_i coincide *at leading logarithmic order* with the Wilson coefficients in the standard basis [7].

As for form factors and non-leptonic two-body decays there exist two distinct classes of non-factorizable effects. (By “non-factorizable” we mean all those corrections that are not contained in the definition of the QCD form factors for heavy-to-light transitions. For example, the familiar leading-order diagrams shown in (a) and (b) of Figure 1 are factorizable.) The first class involves diagrams in which the spectator quark in the B meson participates in the hard scattering. This effect occurs at leading order in an expansion in the strong coupling constant only through a weak annihilation diagram [Figure 1c]. The relevant diagrams at next-to-leading order are shown as (a) and (b) in Figure 2 below and in Figure 3. They contribute at order $\alpha_s^{0,1}$ to the functions T_a in (1). Diagrams of this form have already been considered (for $q^2 = 0$) in [8]. However, bound state model wave-functions (rather than light-cone distribution amplitudes) were used and no attempt was made to systematically expand the hard scattering amplitude in $1/m_b$. As a consequence, the result of [8] for $\bar{B} \rightarrow K^* \gamma$ depends on an infrared cut-off. This difficulty is resolved in the present factorization approach. The second class contains all diagrams shown in the second row of Figure 2 below. Here the spectator quark is connected to the hard process represented by the diagram only through soft interactions. The result is therefore proportional to the form factor ξ_a and the hard-scattering part gives an α_s -correction to the functions C_a in (1).

In this section we present the results of the calculation of these diagrams. Some of the results needed for diagrams of the second class can be extracted from work on inclusive radiative decays [9, 10] and we have made use of these results as indicated below. The conventions for the form factors and light-cone distribution amplitudes for B mesons and light mesons are those of [4].

2.1 Notation and leading-order result

Since the matrix elements of the semi-leptonic operators $\mathcal{O}_{9,10}$ can be expressed through $B \rightarrow K^*$ form factors, non-factorizable corrections contribute to the decay amplitude only through the production of a virtual photon, which then decays into the lepton pair.

We therefore introduce

$$\begin{aligned}
\langle \gamma^*(q, \mu) \bar{K}^*(p', \varepsilon^*) | H_{\text{eff}} | \bar{B}(p) \rangle = & -\frac{G_F}{\sqrt{2}} V_{ts}^* V_{tb} \frac{ig_{\text{em}} m_b}{4\pi^2} \left\{ 2 \mathcal{T}_1(q^2) \epsilon^{\mu\nu\rho\sigma} \varepsilon_\nu^* p_\rho p'_\sigma \right. \\
& -i \mathcal{T}_2(q^2) \left[(M_B^2 - m_{K^*}^2) \varepsilon^{*\mu} - (\varepsilon^* \cdot q) (p^\mu + p'^\mu) \right] \\
& \left. -i \mathcal{T}_3(q^2) (\varepsilon^* \cdot q) \left[q^\mu - \frac{q^2}{M_B^2 - m_{K^*}^2} (p^\mu + p'^\mu) \right] \right\}, \tag{6}
\end{aligned}$$

where H_{eff} denotes the weak effective Hamiltonian. We define the overall quark mass factor as the pole mass here. The matrix element decomposition is defined such that the leading order contribution from the electromagnetic dipole operator \mathcal{O}_7 reads $\mathcal{T}_i(q^2) = C_7 T_i(q^2) + \dots$, where $T_i(q^2)$ denote the tensor form factors. Including also the four-quark operators (but neglecting for the moment annihilation contributions), the leading logarithmic expressions are [11]

$$\mathcal{T}_1(q^2) = C_7^{\text{eff}} T_1(q^2) + Y(q^2) \frac{q^2}{2m_b(M_B + m_{K^*})} V(q^2), \tag{7}$$

$$\mathcal{T}_2(q^2) = C_7^{\text{eff}} T_2(q^2) + Y(q^2) \frac{q^2}{2m_b(M_B - m_{K^*})} A_1(q^2), \tag{8}$$

$$\mathcal{T}_3(q^2) = C_7^{\text{eff}} T_3(q^2) + Y(q^2) \left[\frac{M_B - m_{K^*}}{2m_b} A_2(q^2) - \frac{M_B + m_{K^*}}{2m_b} A_1(q^2) \right], \tag{9}$$

with $C_7^{\text{eff}} = C_7 - C_3/3 - 4C_4/9 - 20C_5/3 - 80C_6/9 = C_7 - (4\bar{C}_3 - \bar{C}_5)/9 - (4\bar{C}_4 - \bar{C}_6)/3$ and

$$\begin{aligned}
Y(s) = & h(s, m_c) (3\bar{C}_1 + \bar{C}_2 + 3\bar{C}_3 + \bar{C}_4 + 3\bar{C}_5 + \bar{C}_6) \\
& - \frac{1}{2} h(s, m_b) (4(\bar{C}_3 + \bar{C}_4) + 3\bar{C}_5 + \bar{C}_6) - \frac{1}{2} h(s, 0) (\bar{C}_3 + 3\bar{C}_4) \\
& + \frac{2}{9} \left(\frac{2}{3} \bar{C}_3 + 2\bar{C}_4 + \frac{16}{3} \bar{C}_5 \right). \tag{10}
\end{aligned}$$

The function

$$h(s, m_q) = -\frac{4}{9} \left(\ln \frac{m_q^2}{\mu^2} - \frac{2}{3} - z \right) - \frac{4}{9} (2+z) \sqrt{|z-1|} \begin{cases} \arctan \frac{1}{\sqrt{z-1}} & z > 1 \\ \ln \frac{1+\sqrt{1-z}}{\sqrt{z}} - \frac{i\pi}{2} & z \leq 1 \end{cases} \tag{11}$$

is related to the basic fermion loop. (Here z is defined as $4m_q^2/s$.) $Y(s)$ is given in the NDR scheme with anticommuting γ_5 and with respect to the operator basis of [6]. Since C_9 is basis-dependent starting from next-to-leading logarithmic order, the terms not proportional to $h(s, m_q)$ differ from those given in [7]. The contributions from the four-quark operators \mathcal{O}_{1-6} are usually combined with the coefficient C_9 into an “effective” (basis- and scheme-independent) Wilson coefficient $C_9^{\text{eff}}(q^2) = C_9 + Y(q^2)$.

The results of this paper are restricted to the kinematic region in which the energy of the final state meson scales with the heavy quark mass in the heavy quark limit. In practice we identify this with the region below the charm pair production threshold $q^2 < 4m_c^2 \approx 7 \text{ GeV}^2$. The various form factors appearing in (7)-(9) are then related by symmetries [5, 4]. Adopting the notation of [4], (7)-(9) simplify to

$$\mathcal{T}_1(q^2) \equiv \mathcal{T}_\perp(q^2) = \xi_\perp(q^2) \left[C_7^{\text{eff}} \delta_1 + \frac{q^2}{2m_b M_B} Y(q^2) \right], \quad (12)$$

$$\mathcal{T}_2(q^2) = \frac{2E}{M_B} \mathcal{T}_\perp(q^2), \quad (13)$$

$$\mathcal{T}_3(q^2) - \frac{M_B}{2E} \mathcal{T}_2(q^2) \equiv \mathcal{T}_\parallel(q^2) = -\xi_\parallel(q^2) \left[C_7^{\text{eff}} \delta_2 + \frac{M_B}{2m_b} Y(q^2) \delta_3 \right], \quad (14)$$

where $E = (M_B^2 - q^2)/(2M_B)$ refers to the energy of the final state meson and $\xi_{\perp,\parallel}$ refer to the form factors in the heavy quark and high energy limit. The factors δ_i are defined such that $\delta_i = 1 + O(\alpha_s)$. The α_s -corrections have been computed in [4] and will be incorporated into the next-to-leading order results later on. The appearance of only two independent structures is a consequence of the chiral weak interactions and helicity conservation, and hence holds also after including next-to-leading order corrections [4, 12]. We therefore present our results in terms of the invariant amplitudes $\mathcal{T}_{\perp,\parallel}(q^2)$, which refer to the decay into a transversely and longitudinally polarized vector meson (virtual photon), respectively. At next-to-leading order we represent these quantities in the form

$$\begin{aligned} \mathcal{T}_a &= \xi_a \left(C_a^{(0)} + \frac{\alpha_s C_F}{4\pi} C_a^{(1)} \right) \\ &+ \frac{\pi^2}{N_c} \frac{f_B f_{K^*,a}}{M_B} \Xi_a \sum_{\pm} \int \frac{d\omega}{\omega} \Phi_{B,\pm}(\omega) \int_0^1 du \Phi_{K^*,a}(u) T_{a,\pm}(u, \omega), \end{aligned} \quad (15)$$

where $C_F = 4/3$, $N_c = 3$, $\Xi_\perp \equiv 1$, $\Xi_\parallel \equiv m_{K^*}/E$, and $T_{a,\pm}(u, \omega)$ is expanded as

$$T_{a,\pm}(u, \omega) = T_{a,\pm}^{(0)}(u, \omega) + \frac{\alpha_s C_F}{4\pi} T_{a,\pm}^{(1)}(u, \omega). \quad (16)$$

$f_{K^*,\parallel}$ denotes the usual K^* decay constant f_{K^*} . $f_{K^*,\perp}$ refers to the (scale-dependent) transverse decay constant defined by the matrix element of the tensor current. The leading-order coefficient $C_a^{(0)}$ follows by comparison with Eqs. (12) and (14) setting $\delta_i = 1$.

To complete the leading-order result we have to compute the weak annihilation amplitude of Figure 1c, which has no analogue in the inclusive decay and generates the hard-scattering term $T_{a,\pm}^{(0)}(u, \omega)$ in (15). To compute this term we perform the projection of the amplitude on the B meson and K^* meson distribution amplitude as explained in [4]. The four diagrams in Figure 1c contribute at different powers in the $1/m_b$ expansion. It turns out that the leading contribution comes from the single diagram with the photon emitted from the spectator quark in the B meson, because this allows the quark propagator to be off-shell by an amount of order $m_b \Lambda_{\text{QCD}}$, the off-shellness being of order m_b^2 for the other three diagrams. With the convention that the K^* meson momentum

is nearly light-like in the minus light-cone direction, the amplitude for the surviving contribution depends only on the minus component of the spectator quark momentum. This is in contrast to the discussion in [4], where, using the same convention for the outgoing meson, the hard-scattering amplitude depended only on the plus component of the spectator quark momentum. As a consequence the B meson distribution amplitude $\Phi_{B,\pm}(\omega)$ now appears as coefficient of \not{n}_{\mp} in the B meson projector. Except for this difference the calculation follows the rules of [4]. The result reads

$$T_{\perp,+}^{(0)}(u, \omega) = T_{\perp,-}^{(0)}(u, \omega) = T_{\parallel,+}^{(0)}(u, \omega) = 0 \quad (17)$$

$$T_{\parallel,-}^{(0)}(u, \omega) = -e_q \frac{M_B \omega}{M_B \omega - q^2 - i\epsilon} \frac{4M_B}{m_b} (\bar{C}_3 + 3\bar{C}_4). \quad (18)$$

At leading order weak annihilation occurs only through penguin operators with small Wilson coefficients. For B^\pm decay, there is an additional Cabibbo-suppressed contribution involving current-current operators, which can be obtained by multiplying the previous equation with the factor

$$- \frac{V_{us}^* V_{ub}}{V_{ts}^* V_{tb}} \cdot \frac{\bar{C}_1 + 3\bar{C}_2}{\bar{C}_3 + 3\bar{C}_4}, \quad (19)$$

whose modulus is about 0.7. Both contributions are numerically small relative to the dominant leading-order terms. Note that since $\mathcal{T}_{\parallel}(q^2)$ does not contribute to the decay amplitude in the limit $q^2 \rightarrow 0$, there is no weak annihilation contribution to $B \rightarrow K^* \gamma$ at leading order in α_s and at leading order in $1/m_b$.

We emphasize that our discussion of weak annihilation refers only to the leading contribution in the heavy quark limit. It is a novel aspect of $B \rightarrow K^* \ell^+ \ell^-$ (with the K^* longitudinally polarized) that weak annihilation does not vanish in this limit, if $q^2 \sim m_b \Lambda_{\text{QCD}}$. On the other hand, the sum of transverse and longitudinal contributions is dominated by the transverse decay amplitude at small q^2 , and it is probable that the power-suppressed annihilation contributions to the transverse amplitude $\mathcal{T}_{\perp}(q^2)$, which we neglected, are numerically more important. For $q^2 = 0$ annihilation contributions of this sort have been studied in [13]. The interplay of the various terms merits consideration for $b \rightarrow d$ transitions, in which weak annihilation through current-current operators is neither CKM- nor α_s -suppressed. Since our main analysis concerns $b \rightarrow s$ decays, we defer this issue to a later discussion.

2.2 Next-to-leading order – spectator scattering

The hard scattering functions $T_{a,\pm}^{(1)}$ in (15) contain a factorizable term from expressing the full QCD form factors in terms of ξ_a , related to the α_s -correction to the δ_i in Eqs. (12), (14) above. We write $T_{a,\pm}^{(1)} = T_{a,\pm}^{(f)} + T_{a,\pm}^{(\text{nf})}$. The factorizable correction reads [4]:

$$T_{\perp,+}^{(f)}(u, \omega) = C_7^{\text{eff}} \frac{2M_B}{\bar{u}E}, \quad (20)$$

$$T_{\parallel,+}^{(f)}(u, \omega) = \left[C_7^{\text{eff}} + \frac{q^2}{2m_b M_B} Y(q^2) \right] \frac{2M_B^2}{\bar{u}E^2} \quad (21)$$

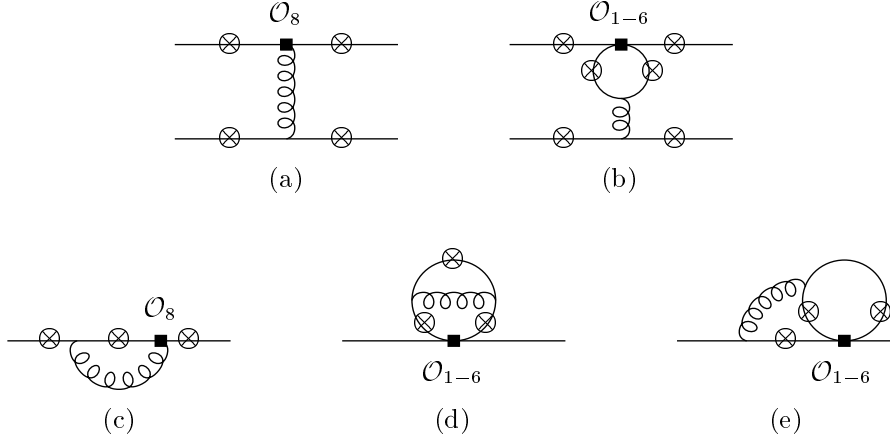


Figure 2: Non-factorizable contributions to $\langle \gamma^* \bar{K}^* | H_{\text{eff}} | \bar{B} \rangle$. The circled cross marks the possible insertions of the virtual photon line. Diagrams that follow from (c) and (e) by symmetry are not shown. Upper line: hard spectator scattering. Lower line: diagrams involving a $B \rightarrow K^*$ form factor (the spectator quark line is not drawn for these diagrams).

$$T_{\perp,-}^{(\text{f})}(u, \omega) = T_{\parallel,-}^{(\text{f})}(u, \omega) = 0 \quad (22)$$

The non-factorizable correction is obtained by computing matrix elements of four-quark operators and the chromomagnetic dipole operator represented by diagrams (a) and (b) in Figure 2. The projection on the meson distribution amplitudes is straightforward. In the result we keep only the leading term in the heavy quark limit, expanding the amplitude in powers of the spectator quark momentum whenever this is permitted by power counting. In practice this means keeping all terms that have one power of the spectator quark momentum in the denominator. Such terms arise either from the gluon propagator that connects to the spectator quark line or from the spectator quark propagator, when the photon is emitted from the spectator quark line. We then find:

$$T_{\perp,+}^{(\text{nf})}(u, \omega) = -\frac{4e_d C_8^{\text{eff}}}{u + \bar{u}q^2/M_B^2} + \frac{M_B}{2m_b} \left[e_u t_{\perp}(u, m_c) (\bar{C}_2 + \bar{C}_4 - \bar{C}_6) \right. \\ \left. + e_d t_{\perp}(u, m_b) (\bar{C}_3 + \bar{C}_4 - \bar{C}_6 - 4m_b/M_B \bar{C}_5) + e_d t_{\perp}(u, 0) \bar{C}_3 \right] \quad (23)$$

$$T_{\perp,-}^{(\text{nf})}(u, \omega) = 0 \quad (24)$$

$$T_{\parallel,+}^{(\text{nf})}(u, \omega) = \frac{M_B}{m_b} \left[e_u t_{\parallel}(u, m_c) (\bar{C}_2 + \bar{C}_4 - \bar{C}_6) + e_d t_{\parallel}(u, m_b) (\bar{C}_3 + \bar{C}_4 - \bar{C}_6) \right. \\ \left. + e_d t_{\parallel}(u, 0) \bar{C}_3 \right] \quad (25)$$

$$T_{\parallel,-}^{(\text{nf})}(u, \omega) = e_q \frac{M_B \omega}{M_B \omega - q^2 - i\epsilon} \left[\frac{8 C_8^{\text{eff}}}{\bar{u} + uq^2/M_B^2} \right. \\ \left. + \frac{6M_B}{m_b} \left(h(\bar{u}M_B^2 + uq^2, m_c) (\bar{C}_2 + \bar{C}_4 + \bar{C}_6) + h(\bar{u}M_B^2 + uq^2, m_b) (\bar{C}_3 + \bar{C}_4 + \bar{C}_6) \right) \right]$$

$$+ h(\bar{u}M_B^2 + uq^2, 0) (\bar{C}_3 + 3\bar{C}_4 + 3\bar{C}_6) - \frac{8}{27} (\bar{C}_3 - \bar{C}_5 - 15\bar{C}_6) \Big]. \quad (26)$$

Here $C_8^{\text{eff}} = C_8 + C_3 - C_4/6 + 20C_5 - 10C_6/3 = C_8 + (4\bar{C}_3 - \bar{C}_5)/3$, $e_u = 2/3$, $e_d = -1/3$ and e_q is the electric charge of the spectator quark in the B meson. $h(s, m_q)$ has been defined above. The functions $t_a(u, m_q)$ arise from the two diagrams of Figure 2b in which the photon attaches to the internal quark loop. They are given by

$$t_\perp(u, m_q) = \frac{2M_B}{\bar{u}E} I_1(m_q) + \frac{q^2}{\bar{u}^2 E^2} (B_0(\bar{u}M_B^2 + uq^2, m_q) - B_0(q^2, m_q)) \quad (27)$$

$$t_\parallel(u, m_q) = \frac{2M_B}{\bar{u}E} I_1(m_q) + \frac{\bar{u}M_B^2 + uq^2}{\bar{u}^2 E^2} (B_0(\bar{u}M_B^2 + uq^2, m_q) - B_0(q^2, m_q)), \quad (28)$$

where B_0 and I_1 are defined as

$$B_0(s, m_q) = -2 \sqrt{4m_q^2/s - 1} \arctan \frac{1}{\sqrt{4m_q^2/s - 1}} \quad (29)$$

$$I_1(m_q) = 1 + \frac{2m_q^2}{\bar{u}(M_B^2 - q^2)} [L_1(x_+) + L_1(x_-) - L_1(y_+) - L_1(y_-)], \quad (30)$$

and

$$x_\pm = \frac{1}{2} \pm \left(\frac{1}{4} - \frac{m_q^2}{\bar{u}M_B^2 + uq^2} \right)^{1/2}, \quad y_\pm = \frac{1}{2} \pm \left(\frac{1}{4} - \frac{m_q^2}{q^2} \right)^{1/2}, \quad (31)$$

$$L_1(x) = \ln \frac{x-1}{x} \ln(1-x) - \frac{\pi^2}{6} + \text{Li}_2 \left(\frac{x}{x-1} \right). \quad (32)$$

The correct imaginary parts are obtained by interpreting m_q^2 as $m_q^2 - i\epsilon$. Closer inspection shows that contrary to appearance none of the hard-scattering functions is more singular than $1/\bar{u}$ as $u \rightarrow 1$. It follows that the convolution integrals with the kaon light-cone distribution are convergent at the endpoints.

The limit $q^2 \rightarrow 0$ ($E \rightarrow M_B/2$) of the transverse amplitude is relevant to the decay $\bar{B} \rightarrow \bar{K}^* \gamma$. The corresponding limiting function reads

$$t_\perp(u, m_q)|_{q^2=0} = \frac{4}{\bar{u}} \left(1 + \frac{2m_q^2}{\bar{u}M_B^2} [L_1(x_+) + L_1(x_-)]|_{q^2=0} \right) \quad (33)$$

In the same limit the longitudinal amplitude develops a logarithmic singularity, which is of no consequence, because the longitudinal contribution to the $\bar{B} \rightarrow \bar{K}^* \ell^+ \ell^-$ decay rate is suppressed by a power of q^2 relative to the transverse contribution in this limit. It does, however, imply that the longitudinal amplitude itself is sensitive to distances of order $1/\sqrt{q^2}$ and not perturbatively calculable unless $q^2 \sim m_b \Lambda_{\text{QCD}}$. (This long-distance sensitivity appears already at leading order in (14) through the light-quark contributions to $Y(q^2)$.)

2.3 Next-to-leading order – form factor correction

The next-to-leading order coefficients $C_a^{(1)}$ in (15) contain a factorizable term from expressing the full QCD form factors in terms of ξ_a , related to the α_s -correction to the δ_i in Eqs. (12), (14). We write $C_a^{(1)} = C_a^{(f)} + C_a^{(\text{nf})}$. The factorizable correction reads [4]:

$$C_{\perp}^{(f)} = C_7^{\text{eff}} \left(4 \ln \frac{m_b^2}{\mu^2} - 4 - L \right), \quad (34)$$

$$C_{\parallel}^{(f)} = -C_7^{\text{eff}} \left(4 \ln \frac{m_b^2}{\mu^2} - 6 + 4L \right) + \frac{M_B}{2m_b} Y(q^2) (2 - 2L) \quad (35)$$

with

$$L \equiv -\frac{m_b^2 - q^2}{q^2} \ln \left(1 - \frac{q^2}{m_b^2} \right). \quad (36)$$

The brackets multiplying C_7^{eff} include the term $3 \ln(m_b^2/\mu^2) - 4$ from expressing the $\overline{\text{MS}}$ quark mass in the definition of the operator \mathcal{O}_7 in terms of the b quark pole mass according to (5). The non-factorizable correction is obtained by computing matrix elements of four-quark operators and the chromomagnetic dipole operator represented by diagrams (c) through (e) in Figure 2.

The matrix elements of four-quark operators require the calculation of two-loop diagrams with several different mass scales. The result for the current-current operators $\mathcal{O}_{1,2}$ is presented in [10] as a double expansion in q^2/m_b^2 and m_c/m_b . Since we are only interested in small q^2 , this result is adequate for our purposes. (Note that only the result corresponding to Figure 1a-e of [10] is needed for our calculation.) The 2-loop matrix elements of penguin operators have not yet been computed and will hence be neglected. Due to the small Wilson coefficients of the penguin operators, this should be a very good approximation. The matrix element of the chromomagnetic dipole operator [Figure 2c] is also given in [10] in expanded form. The exact result is given in Appendix B. All this combined, we obtain

$$C_F C_{\perp}^{(\text{nf})} = -\bar{C}_2 F_2^{(7)} - C_8^{\text{eff}} F_8^{(7)} - \frac{q^2}{2m_b M_B} \left[\bar{C}_2 F_2^{(9)} + 2\bar{C}_1 \left(F_1^{(9)} + \frac{1}{6} F_2^{(9)} \right) + C_8^{\text{eff}} F_8^{(9)} \right], \quad (37)$$

$$C_F C_{\parallel}^{(\text{nf})} = \bar{C}_2 F_2^{(7)} + C_8^{\text{eff}} F_8^{(7)} + \frac{M_B}{2m_b} \left[\bar{C}_2 F_2^{(9)} + 2\bar{C}_1 \left(F_1^{(9)} + \frac{1}{6} F_2^{(9)} \right) + C_8^{\text{eff}} F_8^{(9)} \right]. \quad (38)$$

The quantities $F_{1,2}^{(7,9)}$ can be extracted from [10].¹ The quantities $F_8^{(7,9)}$ are given in Appendix B or can also be extracted from [10] in expanded form. In expressing the result in terms of the coefficients $\bar{C}_{1,2}$, we have made use of $F_1^{(7)} + F_2^{(7)}/6 = 0$. We also substituted C_8 by C_8^{eff} , taking into account a subset of penguin contributions.

¹We thank M. Walker for providing us with additional data points which cover the range $0.25 \leq m_c/m_b \leq 0.35$ needed for the subsequent numerical analysis.

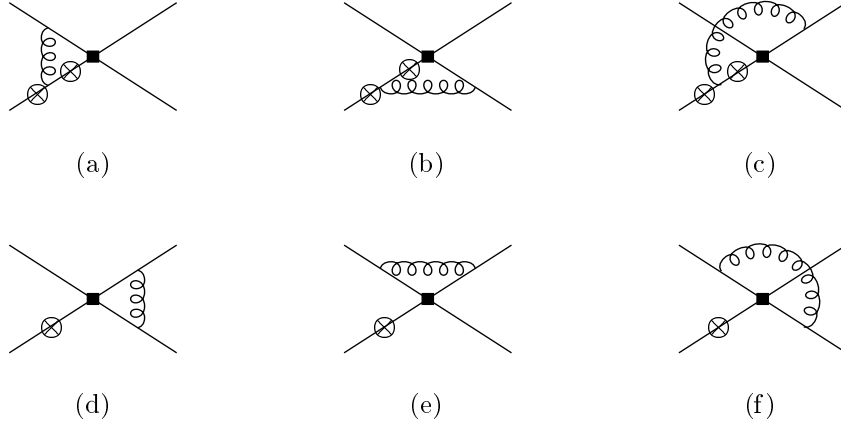


Figure 3: Vertex corrections to the weak annihilation diagram in Figure 1c. Only the photon coupling to the spectator quark line contributes at leading order in $1/m_b$ as indicated by the circled cross.

2.4 Weak annihilation

In addition to the two sets of next-to-leading order corrections discussed up to now, there exist “vertex corrections” to the weak annihilation graph, as shown in Figure 3. The distinction between weak annihilation and the previous spectator scattering diagrams is not clear-cut. The diagrams in Figure 2b with the photon attached to any of the external lines can also pass as a correction to the leading-order weak annihilation graph. In fact, the scale-dependent logarithm in $h(q^2, m_q)$ in (26) cancels part of the scale-dependence of the leading order annihilation amplitude, (17).

For $b \rightarrow s$ transitions current-current operators with large Wilson coefficients cannot be contracted to give diagrams of the type shown in Figure 3. The total contribution is therefore suppressed by three factors: the strong coupling constant; the small Wilson coefficients of QCD penguin operators; and the suppression of the longitudinal amplitude in the decay rate for small q^2 . We shall see subsequently that the leading-order weak annihilation effect is already small. Hence, although the radiative corrections to this leading-order term are of some conceptual interest in connection with renormalization of the B meson distribution amplitude, we shall not include the tiny radiative corrections represented in Figure 3 into our numerical analysis.

2.5 Summary

We now summarize our main result. The matrix element $\langle \gamma^*(q, \mu) \bar{K}^*(p', \varepsilon^*) | H_{\text{eff}} | \bar{B}(p) \rangle$ is not scheme- and scale-independent in the standard operator formalism with an on-shell basis, unless the photon is on-shell. Therefore $\mathcal{T}_{\perp, \parallel}(q^2)$ are not physical quantities. From the expressions for the decay rates given below, it will be clear that the following three quantities are independent of the conventions chosen to renormalize the weak effective Hamiltonian:

$$\mathcal{C}_7 \equiv \frac{\mathcal{T}_{\perp}(0)}{\xi_{\perp}(0)} = C_7^{\text{eff}} + \dots \quad (39)$$

$$\mathcal{C}_{9,\perp}(q^2) \equiv C_9 + \frac{2m_b M_B}{q^2} \frac{\mathcal{T}_\perp(q^2)}{\xi_\perp(q^2)} = C_9 + Y(q^2) + \frac{2m_b M_B}{q^2} C_7^{\text{eff}} + \dots \quad (40)$$

$$\begin{aligned} \mathcal{C}_{9,\parallel}(q^2) \equiv C_9 - \frac{2m_b}{M_B} \frac{\mathcal{T}_\parallel(q^2)}{\xi_\parallel(q^2)} &= C_9 + Y(q^2) + \frac{2m_b}{M_B} C_7^{\text{eff}} - e_q \frac{4M_B}{m_b} (\bar{C}_3 + 3\bar{C}_4) \\ &\times \frac{\pi^2}{N_c} \frac{f_B f_{K^*}}{M_B(E/m_{K^*})\xi_\parallel(q^2)} \int d\omega \frac{M_B \Phi_{B,-}(\omega)}{M_B \omega - q^2 - i\epsilon} + \dots \end{aligned} \quad (41)$$

The quantity $\mathcal{C}_{9,\parallel}(q^2)$ depends on the charge of the B meson through e_q , but this is suppressed in our notation. The ellipses denote the α_s -corrections calculated above and defined through (15). The explicit expressions for the quantities defined in (15) are given in (34)-(38) and (20)-(26). We note that \mathcal{C}_7 , $\mathcal{C}_{9,\perp}$ and $\mathcal{C}_{9,\parallel}$ depend on the conventions adopted in [4] to define the soft form factors ξ_\perp and ξ_\parallel . In addition \mathcal{C}_7 depends also on the b quark mass renormalization scheme (but $m_b \mathcal{C}_7$ does not). We discuss this further after (60) below.

We verified that our results are scale-independent to the required order. More precisely, we have

$$\mu \frac{d}{d\mu} \{ \mathcal{C}_7, \mathcal{C}_{9,\perp}(q^2), \mathcal{C}_{9,\parallel}(q^2) \} = O(\alpha_s^2, \alpha_s C_{3-6}). \quad (42)$$

The uncanceled terms at order α_s are proportional only to the small Wilson coefficients of QCD penguin operators. They are related to the unknown two-loop matrix elements of penguin operators, and to the incomplete evaluation of weak annihilation effects in the case of $\mathcal{C}_{9,\parallel}(q^2)$. Numerically, however, the missing contributions are negligible. When the strong interaction corrections to (39)-(41) are included, the next-to-leading logarithmic expression for C_7^{eff} [6] must be used. However, because $C_9 \sim \ln(M_W/\mu) \sim 1/\alpha_s$ at leading order, the coefficient C_9 is needed to next-to-next-to-leading logarithmic order. The relevant initial conditions for the renormalization group evolution can be taken from [14] and we have incorporated them into our analysis. (The necessary renormalization group formulae are summarized in Appendix C.) However, the three-loop anomalous dimension matrix needed for the evolution is presently not known. Except for this (and the numerically insignificant terms discussed above), our result for $\bar{B} \rightarrow \bar{K}^* \ell^+ \ell^-$ is complete at next-to-next-to-leading logarithmic order.

3 Numerical analysis of \mathcal{C}_7 , $\mathcal{C}_{9,\perp}$, $\mathcal{C}_{9,\parallel}$

3.1 Specification of input parameters

Wilson coefficients. We begin our discussion of input parameters with the Wilson coefficient C_9 , which we need to next-to-next-to-leading logarithmic order. In our analysis we use the complete next-to-next-to-leading logarithmic expression derived in Appendix C, in which we set the unknown 3-loop anomalous dimensions $\kappa^{(1)}$ and $\gamma^{(2)}$ to zero. To estimate the uncertainty this introduces we note that the neglected terms read

$$\delta C_9 = -\frac{a_s(M_W)}{2\beta_0} \left(\kappa^{(1)} D_1(\mu, M_W) + \kappa^{(-1)} D_{-1}(\mu, M_W) V \frac{[V^{-1} \gamma^{(2)T} V]_{ij}}{4\beta_0 + \gamma_i^{(0)} - \gamma_j^{(0)}} V^{-1} \right)_2, \quad (43)$$

Table 1: Wilson coefficients at the scale $\mu = 4.6 \text{ GeV}$ in leading-logarithmic (LL) and next-to-leading-logarithmic order (NLL). Input parameters are $\Lambda_{\overline{\text{MS}}}^{(5)} = 0.220 \text{ GeV}$, $\hat{m}_t(\hat{m}_t) = 167 \text{ GeV}$, $M_W = 80.4 \text{ GeV}$, and $\sin^2\theta_W = 0.23$. 3-loop running is used for α_s . We also give $C_{9,10}$ at NNLL obtained as described in the text.

	\bar{C}_1	\bar{C}_2	\bar{C}_3	\bar{C}_4	\bar{C}_5	\bar{C}_6
LL	-0.257	1.112	0.012	-0.026	0.008	-0.033
NLL	-0.151	1.059	0.012	-0.034	0.010	-0.040
	C_7^{eff}	C_8^{eff}	C_9	C_{10}	C_9^{NNLL}	C_{10}^{NNLL}
LL	-0.314	-0.149	2.007	0	4.214	-4.312
NLL	-0.308	-0.169	4.154	-4.261		

where all notation is defined in Appendix C and the subscript ‘2’ refers to the component of the six-component vector in brackets. Under reasonable assumptions on the pattern of the unknown anomalous dimension matrix (vector) we observe that the largest contribution to the right hand side comes from $\kappa_2^{(1)}$. A rough estimate is therefore

$$\delta C_9 \approx -10^{-3} \kappa_2^{(1)} \left[\left(\frac{\alpha(\mu)}{\alpha(M_W)} \right)^{0.74} - 1 \right]. \quad (44)$$

Allowing $|\kappa_2^{(1)}| < 100$, we conclude that at scales of order of the b quark mass C_9 is known in the Standard Model to an accuracy of about ± 0.1 . (If $\kappa_2^{(1)}$ is much smaller than the upper limit we assume, other terms may dominate δC_9 , but the uncertainty estimate should remain valid.) This is to be compared to an error of ± 0.05 due to the error on the top quark $\overline{\text{MS}}$ mass, $\hat{m}_t(\hat{m}_t) = (167 \pm 5) \text{ GeV}$. The value of C_9 at the scale $\mu = 4.6 \text{ GeV}$ is given in Table 1 together with the remaining Wilson coefficients. The electroweak input parameters that go into these numbers are summarized along with other input parameters in Table 2 below. The strong coupling is always evolved according to the 3-loop formula.

Quark masses. Up to now we have assumed that m_b is the pole mass. It is usually assumed that the pole mass of the b quark is less well known than the $\overline{\text{MS}}$ mass or the potential-subtracted (PS) mass [15]. (The PS mass replaces the pole mass in quantities in which the b quark is nearly on-shell, but has some large infrared contributions removed.) We therefore replace m_b by the PS mass through the relation

$$m_b = m_{b,\text{PS}}(\mu_f) + \frac{4\alpha_s}{3\pi} \mu_f \quad (45)$$

and use $m_{b,\text{PS}}(2 \text{ GeV}) = (4.6 \pm 0.1) \text{ GeV}$ [16] as an input parameter. An exception to this replacement is applied to the function $Y(s)$ in which we keep the b quark pole mass – computed according to (45) – in the small contributions from b quark loops. Apart from reinterpreting m_b as $m_{b,\text{PS}}(2 \text{ GeV})$ the only consequence of introducing the PS mass is

Table 2: Summary of input parameters and estimated uncertainties.

M_W	80.4 GeV	f_B	180 ± 30 MeV
$\hat{m}_t(\hat{m}_t)$	167 ± 5 GeV	$\lambda_{B,+}^{-1}$	(3 ± 1) GeV ⁻¹
$ V_{ts} $	0.041 ± 0.003	$f_{K^*,\perp}(1 \text{ GeV})$	185 ± 10 MeV
α_{em}	1/137	$f_{K^*,\parallel}$	225 ± 30 MeV
$\Lambda_{\text{QCD}}^{(n_f=5)}$	220 ± 40 MeV	$a_1(\bar{K}^*)_{\perp,\parallel}$	0.2 ± 0.1
$m_{b,\text{PS}}(2 \text{ GeV})$	4.6 ± 0.1 GeV	$a_2(\bar{K}^*)_{\perp,\parallel}$	0.05 ± 0.1
m_c	1.4 ± 0.2 GeV	$M_B \xi_{\parallel}(0)/(2m_{K^*})$	0.47 ± 0.09
		$\xi_{\perp}(0)$	0.35 ± 0.07

an additional term $4\mu_f/m_b$ that appears in the round brackets multiplying C_7^{eff} in (34), (35). We use the charm quark pole mass, $m_c = (1.4 \pm 0.2)$ GeV.

Meson parameters. Many of the relevant meson parameters are not directly known from experiment. QCD sum rule calculations substitute for this lack of information and we use [17] as our source of information. A summary of all input parameters together with their assumed errors is given in Table 2. We now discuss some of the input parameters in more detail.

By convention [4] the soft form factors (including the one for a pseudoscalar kaon) at zero momentum transfer are related to the full form factors by

$$\xi_P(0) = F_+^K(0), \quad \xi_{\perp}(0) = \frac{M_B}{M_B + m_{K^*}} V^{K^*}(0), \quad \frac{M_B}{2m_{K^*}} \xi_{\parallel}(0) = A_0^{K^*}(0). \quad (46)$$

to all orders in perturbation theory. For $A_0^{K^*}(0)$ we have taken the QCD sum rule result from [17] and this gives the soft form factor $\xi_{\parallel}(0)$ listed in Table 2. The choice $\xi_{\perp}(0) = 0.35 \pm 0.07$, also given in that Table, requires comment since (46) and $V^{K^*}(0)$ from [17] would give $\xi_{\perp}(0) = 0.39 \pm 0.06$. The motivation for our choice of input is related to the fact that the QCD sum rule prediction for $T_1^{K^*}(0)/V^{K^*}(0)$ deviates from the behaviour expected in the heavy quark limit [4]. An alternative way of computing $\xi_{\perp}(0)$ uses $\xi_{\perp}(0) \approx 0.93 T_1^{K^*}(0)$ (with $T_1^{K^*}(0)$ evaluated at the scale $\mu = m_b$). Taking $T_1^{K^*}(0)$ from [17] gives $\xi_{\perp}(0) \approx 0.35$. Using this smaller input has the advantage that our result for the $\bar{B} \rightarrow \bar{K}^* \gamma$ decay rate is automatically consistent with an alternative representation of this decay rate in terms of the full QCD form factor $T_1^{K^*}(0)$. (This will be discussed in more detail later.) Furthermore, we shall see that the decay rate predicted for $\bar{B} \rightarrow \bar{K}^* \gamma$ at next-to-leading order favours form factors smaller than those estimated with QCD sum rules. We may then take the point of view that $\xi_{\perp}(0)$ is *determined* by $\Gamma(\bar{B} \rightarrow \bar{K}^* \gamma)$ and hence also $T_1^{K^*}(0)$ and $V^{K^*}(0)$ through the relations of [4]. This logic of course implies that we take seriously the heavy quark limit prediction for the decay rate and form factor relations in the heavy quark limit. The energy dependence of the form factors is assumed to be

$$\xi_{\perp}(q^2) = \xi_{\perp}(0) \left(\frac{1}{1 - q^2/M_B^2} \right)^2, \quad \xi_{\parallel}(q^2) = \xi_{\parallel}(0) \left(\frac{1}{1 - q^2/M_B^2} \right)^3, \quad (47)$$

as predicted by power counting in the heavy quark limit.

The hard-spectator scattering (and annihilation) contribution depend on the light-cone wave functions of the B -meson and the light meson in the final state which are characterized in terms of decay constants, Gegenbauer coefficients etc. The leading contribution in the heavy quark mass expansion involves the leading-twist distribution amplitudes of light mesons only. We truncate the expansion of these functions into Gegenbauer-polynomials $C_i^{(3/2)}$ at second order, i.e. ($a = \perp, \parallel$)

$$\Phi_{\bar{K}^*,a}(u) = 6u(1-u) \left\{ 1 + a_1(\bar{K}^*)_a C_1^{(3/2)}(2u-1) + a_2(\bar{K}^*)_a C_2^{(3/2)}(2u-1) \right\} . \quad (48)$$

The values for the Gegenbauer coefficients are taken from [17], but for simplicity we neglect the small differences between $a_i(\bar{K}^*)_\perp$ and $a_i(\bar{K}^*)_\parallel$. We also enlarge the error, see Table 2. In the same Table we also give numerical values for the light meson decay constants [17]. (The Gegenbauer coefficients and the decay constant for a transversely polarized vector meson, f_\perp , are scale-dependent and assumed to be evaluated at the scale 1 GeV. The variation of Gegenbauer moments has a negligible effect on our result compared to the overall parameter uncertainties. We therefore neglect the scale-dependence of the Gegenbauer moments in the numerical analysis, but we evolve f_\perp according to $f_\perp(\mu) = f_\perp(\mu_0) (\alpha_s(\mu)/\alpha_s(\mu_0))^{4/23}$.) The renormalization scale in the hard-scattering and annihilation terms is chosen lower than in the form factor contributions in order to reflect the fact that the typical virtualities in the hard scattering term are of order $m_b \Lambda_{\text{QCD}}$ rather than m_b^2 . If μ_1 (assumed to be of order m_b) is the scale in the form factor term, we choose $(\mu_1 \Lambda_h)^{1/2}$ with $\Lambda_h = 0.5 \text{ GeV}$ in the hard-scattering term. This convention applies to all scale-dependent quantities in the hard-scattering term including α_s and the Wilson coefficients.

The two B meson light-cone distribution amplitudes enter only through the two “moments”

$$\lambda_{B,+}^{-1} = \int_0^\infty d\omega \frac{\Phi_{B,+}(\omega)}{\omega} , \quad (49)$$

$$\lambda_{B,-}^{-1}(q^2) = \int_0^\infty d\omega \frac{\Phi_{B,-}(\omega)}{\omega - q^2/M_B - i\epsilon} \quad (50)$$

The moment of $\Phi_{B,+}$ is identical to the moment that appears also in non-leptonic B decays [2], the decay $B \rightarrow \gamma l \nu$ [18] and in the factorization of form factors [4]. The appearance of $\Phi_{B,-}$ at leading order in the heavy quark expansion is a new aspect of the decay $\bar{B} \rightarrow \bar{K}^* \ell^+ \ell^-$.

The light-cone distribution amplitudes $\Phi_{B,\pm}(\omega)$ appearing in (49), (50) are not well-constrained at present and provide a major source of uncertainty in our calculation. Some general properties have been derived in the literature [4, 19]. The equations of motions for the light quark in the B -meson lead to

$$\Phi_{B,-}(\omega) = \int_0^1 \frac{d\eta}{\eta} \Phi_{B,+}(\omega/\eta) \quad \Leftrightarrow \quad \Phi_{B,+}(\omega) = -\omega \Phi'_{B,-}(\omega) \quad (51)$$

We conclude from this that $\lambda_{B,+}^{-1} = \Phi_{B,-}(0)$. Furthermore $\lambda_{B,-}^{-1}(q^2)$ must diverge loga-

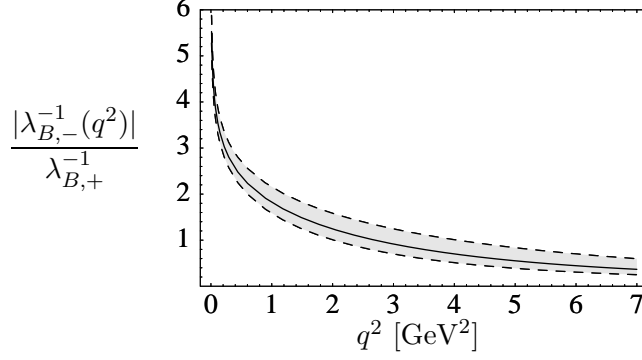


Figure 4: The absolute value of the ratio of B -meson moments $|\lambda_{B,-}^{-1}(q^2)|/\lambda_{B,+}^{-1}$ as a function of q^2 . The B -meson distribution amplitudes are taken as in (53) with $\omega_0^{-1} = (3 \pm 1) \text{ GeV}^{-1}$.

rithmically for $q^2 \rightarrow 0$, provided that $\lambda_{B,+}^{-1} \neq 0$:

$$\lim_{q^2 \rightarrow 0} \lambda_{B,-}^{-1}(q^2) = \lambda_{B,+}^{-1} \int_0^1 \frac{d\eta}{\eta} \rightarrow \infty \quad (52)$$

On the other hand, for $q^2 = O(M_B \Lambda_{\text{QCD}})$ the moment $\lambda_{B,-}^{-1}(q^2)$ is finite and of order $1/\Lambda_{\text{QCD}}$. The equations of motion for the heavy quark relate the first moments $\langle \omega \rangle_{B,\pm}$ to the mass difference $\bar{\Lambda}_{\text{HQET}} = M_B - m_b$, leading to $\langle \omega \rangle_{B,+} = 2\langle \omega \rangle_{B,-} = 4\bar{\Lambda}_{\text{HQET}}/3$. For $\lambda_{B,+}$ the upper bound $4\bar{\Lambda}_{\text{HQET}}/3$ has been derived in [18]. The simple model functions

$$\Phi_{B,+}(\omega) = \frac{\omega}{\omega_0^2} e^{-\omega/\omega_0}, \quad \Phi_{B,-}(\omega) = \frac{1}{\omega_0} e^{-\omega/\omega_0} \quad (53)$$

with $\omega_0 = 2\bar{\Lambda}_{\text{HQET}}/3$, that have been proposed in [19], are consistent with these general constraints, leading to $\lambda_{B,+} = 2\bar{\Lambda}_{\text{HQET}}/3$, and

$$\lambda_{B,-}^{-1}(q^2) = \frac{e^{-q^2/(M_B \omega_0)}}{\omega_0} \left[-\text{Ei}(q^2/M_B \omega_0) + i\pi \right] \quad (54)$$

where $\text{Ei}(z)$ is the exponential integral function. Numerically, for $\bar{\Lambda}_{\text{HQET}} \simeq 500 \text{ MeV}$, one obtains $\lambda_{B,+}^{-1} \simeq 3 \text{ GeV}^{-1}$ with an estimated error of about 1 GeV^{-1} . For the same parameter values the absolute value of $\lambda_{B,-}^{-1}(q^2)$, normalized to $\lambda_{B,+}^{-1}$ is plotted in Figure 4. There exist alternative proposals for B -meson light-cone wave functions, for instance from the Bauer-Stech-Wirbel model [20] or variants of it. Since in these models the distinction between $\Phi_{B,+}(\omega)$ and $\Phi_{B,-}(\omega)$ is not made, we refrain from presenting a thorough comparison of different models and stick to (54) to evaluate the moment of $\Phi_{B,-}(\omega)$. This means that we neglect a systematic uncertainty related to the *shape* of $\Phi_{B,-}(\omega)$, but this uncertainty is irrelevant numerically, because the moment in question appears only in the small annihilation contribution and the small correction to $\mathcal{C}_{9,\parallel}(q^2)$.

All input values from the meson sector together with their estimated uncertainties are summarized in Table 2. We note that apart from the renormalization scale uncertainty

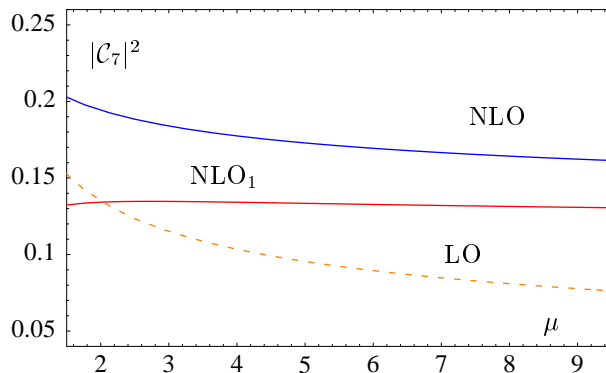


Figure 5: Renormalization scale-dependence of $|\mathcal{C}_7|^2$ at leading (LO) and next-to-leading order (NLO). The curve “NLO₁” shows the NLO result without the spectator scattering correction.

and the error in our knowledge of α_s , the most important uncertain parameters can be collected into a single factor

$$\frac{\pi^2 f_B f_{K^*,a}}{N_c M_B \lambda_{B,+} \xi_a(0)} \quad (55)$$

that determines the relative magnitude of the hard-scattering versus the form factor term. Adding all errors in quadrature, this factor is uncertain by about $\pm 50\%$, where the largest error is currently from $\lambda_{B,+}^{-1}$.

3.2 Exclusive effective “Wilson” coefficients

Having specified our numerical input, we now discuss the three effective “Wilson” coefficients \mathcal{C}_7 , $\mathcal{C}_{9,\perp}(q^2)$ and $\mathcal{C}_{9,\parallel}(q^2)$.

We begin with the quantity $|\mathcal{C}_7|^2$ to which the decay rate of $\bar{B} \rightarrow \bar{K}^* \gamma$ is proportional. In Figure 5 we show the renormalization scale dependence of this quantity at leading and at next-to-leading order. We also show a curve that corresponds to setting the hard-scattering term to zero, i.e. to taking into account only the correction $C_a^{(1)}$ in (15). The reason for considering this term separately is that it should cancel the sizeable leading-order scale dependence, while the hard scattering correction is a physically different effect that appears first at next-to-leading order. Figure 5 shows that this is indeed correct. The hard scattering correction reintroduces a mild scale-dependence. The most important effect is however a large enhancement of $|\mathcal{C}_7|^2$ at next-to-leading order. At the scale $m_b = 4.6 \text{ GeV}$ we find

$$|\mathcal{C}_7|_{\text{NLO}}^2 / |\mathcal{C}_7|_{\text{LO}}^2 \approx 1.78, \quad (56)$$

which corresponds to a sizeable, but not unreasonable 33% correction on the amplitude level. The form factor and hard-scattering correction contribute about equally to this enhancement. More precisely, the [non-]factorizable part of $C_{\perp}^{(1)}$ (defined in (15)) is a -8% [$+24\%$] correction to the real part of the amplitude, the [non-]factorizable part of $T_{\perp,+}^{(1)}$ is a $+11\%$ [$+5\%$] correction (all numbers at $\mu = m_b$). The error on $|\mathcal{C}_7|^2$ is

estimated by combining in quadrature the error from all input parameters as specified in the previous section and from allowing the renormalization scale to vary from $m_b/2$ to $2m_b$. (The scale in the hard scattering term is accordingly lower, see the discussion above.). The result is

$$|\mathcal{C}_7|_{\text{NLO}}^2 = 0.175_{-0.026}^{+0.029}, \quad (57)$$

where the largest errors are from scale dependence (± 0.014), $\lambda_{B,+}^{-1}$ (± 0.015), $\xi_{\perp}(0)$ (± 0.009), and Λ_{QCD} (± 0.010). The value given refers to using the PS mass $m_{b,\text{PS}}(2 \text{ GeV})$, since only the product $m_{b,\text{PS}}(2 \text{ GeV}) |\mathcal{C}_7|$ is convention-independent. The NLO result for $|\mathcal{C}_7|^2$ must be compared to $|\mathcal{C}_7|_{\text{LO}}^2 = 0.098$ with a 30% error from scale dependence alone. At this place it is also appropriate to note that our result is based on the heavy quark expansion, and therefore there exist corrections of order Λ_{QCD}/m_b at the amplitude level. At present we have no means of quantifying these corrections in a systematic way.

The q^2 -dependent coefficients $\mathcal{C}_{9,\perp}(q^2)$, $\mathcal{C}_{9,\parallel}(q^2)$ defined in (40), (41) are shown in Figure 6. The left panels display the reduction of renormalization scale dependence in going from leading order to next-to-leading order (including the intermediate approximation with the hard scattering term set to zero). The right panel gives the complete NLO result with all input parameter uncertainties and scale dependence included in the error estimate.

The characteristic features of the result can be understood from the discussion of \mathcal{C}_7 above. Since $C_9 > 0$ and $C_7^{\text{eff}} < 0$, the contribution to $\mathcal{C}_{9,a}(q^2)$ from the virtual photon matrix element, $\mathcal{T}_a(q^2)$, is always negative ($a = \perp, \parallel$). In the case of a transverse virtual photon, this contribution is enhanced by a factor M_B^2/q^2 owing to the real photon pole and hence dominates $\mathcal{C}_{9,\perp}$ at small q^2 . This causes $\text{Re}(\mathcal{C}_{9,\perp})$ to change its sign and results in the characteristic shape of $|\mathcal{C}_{9,\perp}|$. Due to the large contribution from the photon pole the next-to-leading order contribution is again substantial and the value of momentum transfer q_0^2 at which $\text{Re}(\mathcal{C}_{9,\perp})$ changes its sign is increased. Since q_0^2 determines the location of the forward-backward asymmetry zero, this important correction will be discussed in some detail in Section 5.2. The photon pole is absent in the longitudinal coefficient $\mathcal{C}_{9,\parallel}$, so the NLO correction to it is much smaller. The form factor and hard scattering correction (both small) nearly compensate each other leaving no net modification of the leading order coefficient. Contrary to the transverse coefficient, the longitudinal one depends on the charge of the spectator quark in the B meson, i.e. on the charge of the decaying B meson. This effect is already present at leading order via the annihilation contribution. At NLO it amounts to a few percent of $\mathcal{C}_{9,\parallel}$, the precise magnitude being q^2 -dependent. We return to a discussion of this isospin-breaking effect in the context of the $\bar{B} \rightarrow \bar{K}^* \ell^+ \ell^-$ decay spectrum.

The peculiar discontinuity in the error band around $q^2 = 6 \text{ GeV}^2$ in two of the right panels of Figure 6 is unphysical and related to the fact that in computing the error we allow the charm quark mass to be as small as 1.2 GeV . The discontinuity is a consequence of the $c\bar{c}$ threshold in the charm loop diagrams and reminds us that the validity of our calculation is not only limited by the requirement that the K^* momentum is large (which puts an upper bound on q^2), but also by the lack of a model-independent treatment of the resonant charmonium contributions. The physical “threshold” begins at $M_{J/\psi}^2 \approx 9.6 \text{ GeV}^2$, but the perturbative approximation is expected to fail earlier. Model-dependent studies of the charmonium contributions suggest that the perturbative

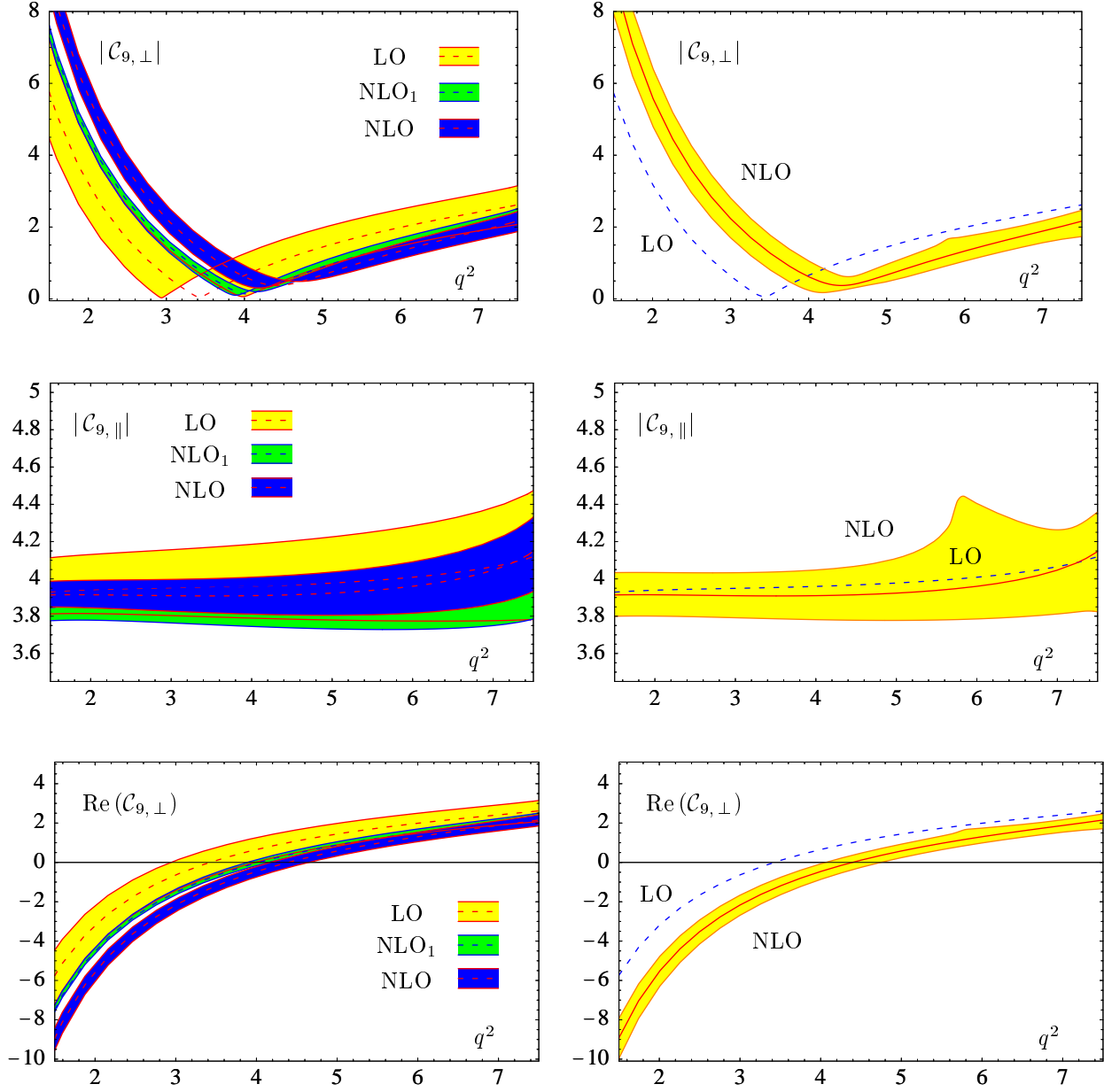


Figure 6: Momentum-transfer dependence of $|\mathcal{C}_{9,\perp}|$, $|\mathcal{C}_{9,\parallel}|$ and $\text{Re}(\mathcal{C}_{9,\perp})$. The left panels show the LO, NLO and NLO result without spectator scattering (“NLO₁”) for fixed input parameters. The width of the bands demonstrates the renormalization scale dependence estimated by variation from $m_b/2$ to $2m_b$. The right panel shows the next-to-leading order result including renormalization scale and input parameter uncertainties (all added in quadrature), and for comparison the leading order result (dashed). The solid line in the center of the band refers to the NLO result with default parameters. $|\mathcal{C}_{9,\parallel}|$ is given for B^- mesons.

approximation should be valid up to $q^2 \approx (6 - 7) \text{ GeV}^2$ [21, 22]. (This supposes that we discard a charm mass as small as 1.2 GeV in estimating effects related to the charm threshold.)

4 The decay $\bar{B} \rightarrow \bar{K}^* \gamma$

The decay rate for $\bar{B} \rightarrow \bar{K}^* \gamma$ in the heavy quark limit is given by

$$\Gamma(\bar{B} \rightarrow \bar{K}^* \gamma) = \frac{G_F^2 |V_{ts}^* V_{tb}|^2}{8\pi^3} M_B^3 \left(1 - \frac{m_{K^*}^2}{M_B^2}\right)^3 \frac{\alpha_{\text{em}}}{4\pi} m_{b,\text{PS}}^2 \xi_\perp(0)^2 |\mathcal{C}_7|^2, \quad (58)$$

with $m_{b,\text{PS}} \equiv m_{b,\text{PS}}(2 \text{ GeV})$ the PS mass. We included the kaon mass squared in a phase space and kinematic correction, but we generally neglect such terms in the dynamical quantity $\mathcal{T}_\perp(0) = \xi_\perp(0) \mathcal{C}_7$. By helicity conservation the kaon is transversely polarized and only the transverse soft form factor $\xi_\perp(0)$ appears in the decay rate. In numerical form, the branching fraction is

$$\text{Br}(\bar{B} \rightarrow \bar{K}^* \gamma) = (7.9_{-1.6}^{+1.8}) \cdot 10^{-5} \left(\frac{\tau_B}{1.6 \text{ ps}}\right) \left(\frac{m_{b,\text{PS}}}{4.6 \text{ GeV}}\right)^2 \left(\frac{\xi_\perp(0)}{0.35}\right)^2 = (7.9_{-3.0}^{+3.5}) \cdot 10^{-5} \quad (59)$$

using $|\mathcal{C}_7|^2 = 0.175_{-0.026}^{+0.029}$ and $m_{b,\text{PS}} = (4.6 \pm 0.1) \text{ GeV}$, $\xi_\perp(0) = 0.35 \pm 0.07$, $|V_{ts}| = 0.041 \pm 0.003$, $\alpha_{\text{em}} = 1/137$, as in Table 2. (τ_B denotes the B meson lifetime.) For comparison we note that the leading order prediction is $4.5 \cdot 10^{-5}$. The large difference reflects the enhancement of $|\mathcal{C}_7|^2$ at next-to-leading order as discussed in Section 3.2. The branching ratio predicted for the default parameter set is nearly twice as large as the current experimental averages [23, 24, 25]

$$\text{Br}(\bar{B}^0 \rightarrow \bar{K}^{*0} \gamma)_{\text{exp}} = (4.54 \pm 0.37) \cdot 10^{-5}, \quad (60)$$

$$\text{Br}(B^- \rightarrow \bar{K}^{*-} \gamma)_{\text{exp}} = (3.81 \pm 0.68) \cdot 10^{-5}. \quad (61)$$

Note that we predict no difference of the neutral and charged B meson decay rates at leading order in the heavy quark expansion, so that the main effect of isospin breaking on branching fractions is the different lifetimes of the charged and neutral mesons.

Before speculating on the origin of this discrepancy, we note that there are alternative ways of representing the result of our calculation. Since the decay amplitude is proportional to a single form factor, $T_1^{K^*}(0)$, there is no need to introduce the soft form factor $\xi_\perp(0)$, and we can express the decay rate directly in terms of the full QCD form factor. (The need to introduce the soft form factors arises when we consider the $\bar{K}^* \ell^+ \ell^-$ final state, which involves many form factors that all relate to the same soft form factors.) Furthermore the dominant dependence on the b quark mass arises through the factor m_b in the definition of the operator \mathcal{O}_7 , so it is also more natural to keep the $\overline{\text{MS}}$ mass $\hat{m}_b(\hat{m}_b)$ as a prefactor rather than the PS mass. This alternative representation amounts to a redefinition of \mathcal{C}_7 in which all *factorizable* corrections vanish at the scale \hat{m}_b , if we understand $T_1^{K^*}(0)$ as renormalized at the scale \hat{m}_b . We have computed the coefficient

\mathcal{C}'_7 also in this alternative scheme (indicated by the prime) and find that (58) is modified as follows:

$$\begin{aligned} m_{b,\text{PS}}^2 \xi_\perp(0)^2 |\mathcal{C}_7|^2 &\longrightarrow \hat{m}_b(\hat{m}_b)^2 T_1^{K*}(0)^2 |\mathcal{C}'_7|^2 \\ |\mathcal{C}_7|^2 = 0.175^{+0.029}_{-0.026} &\longrightarrow |\mathcal{C}'_7|^2 = 0.165^{+0.018}_{-0.017} \end{aligned} \quad (62)$$

The error is smaller in the primed scheme, because the hard-scattering correction is much reduced once the factorizable correction is reabsorbed into the full QCD form factor. This implies less sensitivity to the uncertain parameters that normalize this correction. The two values given in (62) are consistent with each other if one relates $T_1^{K*}(0) = 1.08 \xi_\perp(0)$ [4] and takes into account that $m_{b,\text{PS}}(2 \text{ GeV}) = 4.6 \text{ GeV}$ corresponds to $\hat{m}_b(\hat{m}_b) = 4.4 \text{ GeV}$.

Several facts may explain the difference between the predicted and observed decay rate. The first and most interesting possibility is a modification of the standard model at short distances that would result in a smaller value of $|\mathcal{C}_7|$. However, the modification needed to explain the observed decay rate is far too large not to be ruled out by the agreement between experiment and theory for the *inclusive* decay $\bar{B} \rightarrow X_s \gamma$. It appears equally implausible that new interactions would modify only the spectator scattering and hence not show up in the inclusive rate. We therefore conclude that the explanation must be sought in our understanding of QCD effects. Most of the NLO enhancement is related to the non-factorizable form factor type correction which appears in a nearly identical form in the inclusive decay rate as well. Hence this enhancement cannot be simply dismissed without putting the agreement for the inclusive decay into question. A second and less interesting possibility is therefore to invoke a large $1/m_b$ correction that would render our calculation unreliable. Given the smallness of the non-factorizable hard scattering correction it is not obvious how such a large dynamical enhancement of $1/m_b$ terms could be explained. This is in particular so as large $1/m_b$ corrections known to exist for non-leptonic decays [2, 26] such as “chirally enhanced” corrections and large weak annihilation contributions are absent for decays into vector mesons.

We therefore consider seriously the possibility that the form factors at $q^2 = 0$ are substantially different from what they are assumed to be in the QCD sum rule approach or in quark models. This possibility is entertained in Figure 7, where we show how the experimental data constrains the soft form factor $\xi_\perp(0)$ and the normalization of the hard scattering term. (We take all parameters other than $\lambda_{B,+}^{-1}$ in the normalizing factor constant and let $\lambda_{B,+}^{-1}$ be a representative. That is, a variation of $\lambda_{B,+}^{-1}$ should be considered as a variation of a combination of parameters of the type (55). All other parameter uncertainties are approximately accounted for by adding a 20% uncertainty to the measured branching fraction which we combine with the experimental error in quadrature.) The result of this fit is that

$$T_1^{K*}(0)|_{\mu=m_b} = 0.27 \pm 0.04 \quad [\xi_\perp(0) = 0.24 \pm 0.06], \quad (63)$$

where the error may be loosely interpreted as a one standard deviation error. This determination yields a smaller form factor than a similar determination in [12], where the NLO correction is not included and the bottom quark mass is handled differently.

Our results can be extended in a straightforward way to the decay $\bar{B} \rightarrow \rho \gamma$. This decay is particularly interesting in searches for extensions of the standard model, because

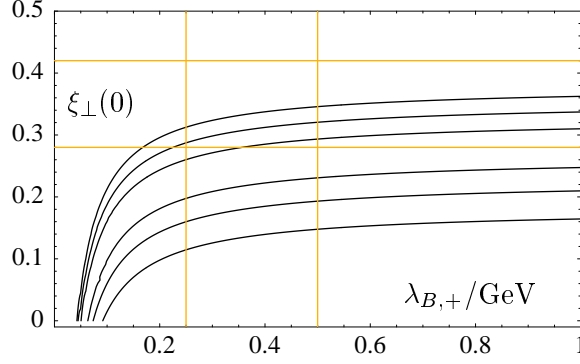


Figure 7: Fit to $\xi_{\perp}(0)$ and $\lambda_{B,+}$. The solid curves give the 1σ , 2σ and 3σ regions that follow from the observed $\bar{B} \rightarrow \bar{K}^* \gamma$ decay rate. The light solid curves mark the ranges assumed for $\xi_{\perp}(0)$ and $\lambda_{B,+}$ in Table 2.

of the suppression of $b \rightarrow d$ transitions in the standard model and the simultaneous chirality suppression. Except for trivial adjustments the most important difference to the $\bar{K}^* \gamma$ final state is that the different flavour structure allows weak annihilation to proceed through the current-current operator with large Wilson coefficient \bar{C}_2 . This annihilation contribution is power-suppressed in $1/m_b$, but the suppression is compensated by the large Wilson coefficient and the occurrence of annihilation at tree level. The annihilation contribution is calculable and has to be taken into account in a realistic analysis [13, 27]. This will be done elsewhere [28, 29], and we restrict ourselves to $b \rightarrow s$ transitions in this paper.

5 The decay $\bar{B} \rightarrow \bar{K}^* \ell^+ \ell^-$

For the decay $\bar{B} \rightarrow \bar{K}^* \ell^+ \ell^-$ we obtain the double differential decay spectrum (summed over final state polarisations, and lepton masses neglected)

$$\begin{aligned}
\frac{d^2\Gamma}{dq^2 d\cos\theta} = & \frac{G_F^2 |V_{ts}^* V_{tb}|^2}{128\pi^3} M_B^3 \lambda(q^2, m_{K^*}^2)^3 \left(\frac{\alpha_{\text{em}}}{4\pi} \right)^2 \\
& \left[(1 + \cos^2\theta) \frac{2q^2}{M_B^2} \xi_{\perp}(q^2)^2 (|\mathcal{C}_{9,\perp}(q^2)|^2 + C_{10}^2) \right. \\
& + (1 - \cos^2\theta) \left(\frac{E \xi_{\parallel}(q^2)}{m_{K^*}} \right)^2 (|\mathcal{C}_{9,\parallel}(q^2)|^2 + C_{10}^2 \Delta_{\parallel}(q^2)^2) \\
& \left. - \cos\theta \frac{8q^2}{M_B^2} \xi_{\perp}(q^2)^2 \text{Re}(\mathcal{C}_{9,\perp}(q^2)) C_{10} \right], \tag{64}
\end{aligned}$$

where

$$\lambda(q^2, m_{K^*}^2) = \left[\left(1 - \frac{q^2}{M_B^2} \right)^2 - \frac{2m_{K^*}^2}{M_B^2} \left(1 + \frac{q^2}{M_B^2} \right) + \frac{m_{K^*}^4}{M_B^4} \right]^{1/2}, \tag{65}$$

and q^2 is the invariant mass of the lepton pair. The angle θ refers to the angle between the positively charged lepton and the B meson in the center-of-mass frame of the lepton pair. We have kept terms of order $m_{K^*}^2$ in an overall factor related to phase space and kinematics but emphasize that the expression in brackets neglects such terms. The first two terms with angular dependence $(1 \pm \cos^2 \theta)$ correspond to the production of transversely and longitudinally polarized kaons, respectively. The third term generates a forward-backward asymmetry with respect to the plane perpendicular to the lepton momentum in the center-of-mass frame of the lepton pair. The factor Δ_{\parallel} multiplying the Wilson coefficient C_{10} in (64) arises from the factorizable corrections to the form-factor A_2 and is given by (cf. Eq. (66) in [4])

$$\Delta_{\parallel}(q^2) = 1 + \frac{\alpha_s C_F}{4\pi} (-2 + 2L) - \frac{\alpha_s C_F}{4\pi} \frac{2q^2}{E^2} \frac{\pi^2 f_B f_{K^* \parallel} \lambda_{B+}^{-1}}{N_c M_B (E/m_{K^*}) \xi_{\parallel}(q^2)} \int_0^1 \frac{du}{u} \Phi_{\parallel}(u) \quad (66)$$

with L defined in (36) and $E = (M_B^2 - q^2)/(2M_B)$. (This factor could be eliminated by choosing a factorization convention different from (46) for the soft form factor ξ_{\parallel} and by redefining $\mathcal{C}_{9,\parallel}$ accordingly.)

Without going into much detail, we remark that the result for the decay into pseudoscalar mesons, $\bar{B} \rightarrow \bar{K} \ell^+ \ell^-$, is easily obtained from the corresponding expressions for the decay into longitudinally polarized vector mesons. The angular distribution is predicted to be proportional to $(1 - \cos^2 \theta)$ and for the lepton invariant mass spectrum we obtain

$$\frac{d\Gamma}{dq^2} = \frac{G_F^2 |V_{ts}^* V_{tb}|^2}{96\pi^3} M_B^3 \lambda(q^2, m_K^2)^3 \left(\frac{\alpha_{\text{em}}}{4\pi} \right)^2 \xi_P(q^2)^2 (|\mathcal{C}_{9,P}(q^2)|^2 + C_{10}^2) \quad (67)$$

where the quantities analogous to those in (6), (40) are now defined as

$$\mathcal{C}_{9,P}(q^2) = C_9 + \frac{2m_b}{M_B} \frac{\mathcal{T}_P(q^2)}{\xi_P(q^2)}, \quad (68)$$

and

$$\langle \gamma^*(q, \mu) \bar{K}(p') | H_{\text{eff}} | \bar{B}(p) \rangle = \frac{G_F}{\sqrt{2}} V_{ts}^* V_{tb} \frac{g_{\text{em}} m_b}{4\pi^2} \frac{\mathcal{T}_P(q^2)}{M_B} \left[q^2 (p^\mu + p'^\mu) - (M_B^2 - m_K^2) q^\mu \right]. \quad (69)$$

The non-factorizable contributions to \mathcal{T}_P are the same as those to \mathcal{T}_{\parallel} up to an overall sign and the replacement $\Xi_{\parallel} f_{K,\parallel} \Phi_{K^*,\parallel}(u) \rightarrow f_K \Phi_K(u)$ in (15). The factorizable contributions follow from the ratio of the tensor form factor $f_T(q^2)$ and the soft form factor $\xi_P(q^2)$ as calculated in [4]. The net result for $\mathcal{C}_{9,P}$ is then

$$\mathcal{C}_{9,P}(q^2) = \frac{\mathcal{C}_{9,\parallel}(q^2)}{\Delta_{\parallel}(q^2)}, \quad (70)$$

where the replacements $\Xi_{\parallel} f_{K,\parallel} \Phi_{K^*,\parallel}(u) \rightarrow f_K \Phi_K(u)$, $\xi_{\parallel}(q^2) \rightarrow -\xi_P(q^2)$ are understood to be performed on the right-hand side.

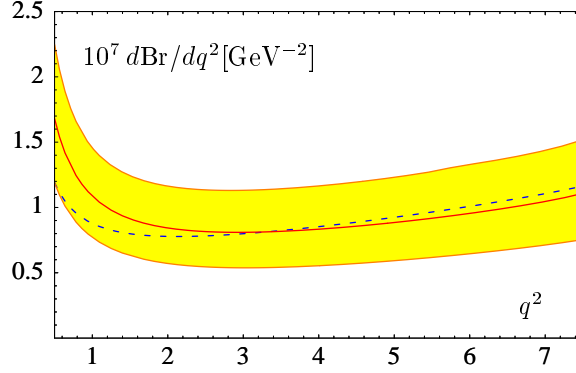


Figure 8: Differential decay rate $d\text{Br}(B^- \rightarrow K^{*-}\ell^+\ell^-)/dq^2$ at next-to-leading order (solid center line) and leading order (dashed). The band reflects all theoretical uncertainties from parameters and scale dependence combined, with most of the uncertainty due to the form factors $\xi_{\perp,\parallel}(0)$.

5.1 Lepton invariant mass spectrum

The lepton invariant mass spectrum $d\text{Br}/dq^2$, obtained by integrating (64) over $\cos\theta$, is shown in Figure 8. (We use the B meson lifetime $\tau_{B^-} = 1.65\text{ps.}$) As the decay rate is dominated by the contribution of longitudinally polarized K^* mesons and the contribution from \mathcal{O}_{10} except for small q^2 , the impact of the next-to-leading order correction is small for $q^2 > 2\text{GeV}^2$. (This can be directly inferred from the small correction to $|\mathcal{C}_{9,\parallel}|$ as seen in Figure 6.) The apparently rather large uncertainty of our prediction is mainly due to the form factors with their current large uncertainty and to a lesser extent due to $|V_{ts}|$ and the top quark mass. It may be hoped that in the longer term future the form factors could be known with much greater confidence. The uncertainties can then be reduced by a factor of three in which case the limiting factor of our prediction is probably $1/m_b$ corrections, all other parameter and scale variations being negligible in comparison.

Since $|\mathcal{C}_{9,\parallel}|$ depends on the charge of the decaying B meson, there is a small amount of isospin breaking. While this effect is q^2 -dependent for $|\mathcal{C}_{9,\parallel}|$, the combination of coefficients that enters the lepton invariant mass spectrum turns out to be almost independent on q^2 . The effect is, however, very small,

$$\delta = \frac{d\Gamma(B^- \rightarrow K^{*-}\ell^+\ell^-)/dq^2 - d\Gamma(\bar{B}^0 \rightarrow \bar{K}^{*0}\ell^+\ell^-)/dq^2}{d\Gamma(B^- \rightarrow K^{*-}\ell^+\ell^-)/dq^2 + d\Gamma(\bar{B}^0 \rightarrow \bar{K}^{*0}\ell^+\ell^-)/dq^2} \approx 1\%. \quad (71)$$

For the differential branching fractions the main isospin breaking effect arises from the lifetime difference of the charged and neutral B mesons.

The impact of the NLO correction on the lepton invariant mass spectrum to the decay in a pseudoscalar meson follows a qualitatively similar pattern as for the vector meson final state, in particular as the decay rate involves only a quantity closely related to $|\mathcal{C}_{9,\parallel}|$ (see (70)). We therefore do not discuss this decay in further detail here, but note that the lepton invariant mass spectrum develops a logarithmic singularity for small q^2 . This is due to the long-distance sensitivity mentioned above, which is now dominant because the photon pole is absent. The invariant mass spectrum is therefore non-perturbative

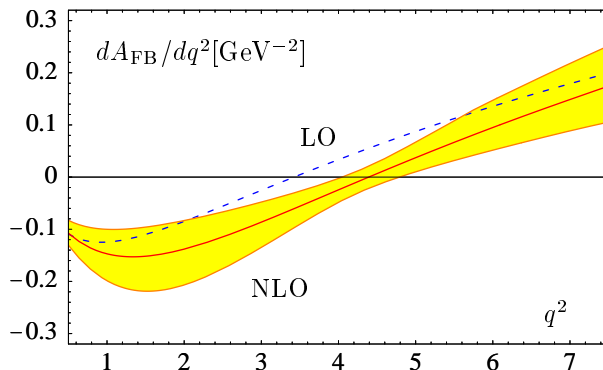


Figure 9: Forward-backward asymmetry $dA_{\text{FB}}(B^- \rightarrow K^{*-}\ell^+\ell^-)/dq^2$ at next-to-leading order (solid center line) and leading order (dashed). The band reflects all theoretical uncertainties from parameters and scale dependence combined.

for $q^2 \sim \Lambda_{\text{QCD}}^2$, but perturbative for $q^2 \sim m_b \Lambda_{\text{QCD}}$. Furthermore, the non-perturbative contribution is formally power-suppressed when the lepton invariant mass spectrum is integrated from 0 to some q^2 of order $m_b \Lambda_{\text{QCD}}$.

5.2 Forward-backward asymmetry

The QCD factorization approach proposed here leads to an almost model-independent theoretical prediction for the forward-backward asymmetry [30]. It has been noted in [31] that the location of the forward-backward asymmetry zero is nearly independent of particular form factor models. An explanation of this fact was given in [32], where it has been noted that the form factor ratios on which the asymmetry zero depends are predicted free of hadronic uncertainties in the combined heavy quark and large energy limit. In [4] the effect of the (factorizable) radiative corrections to the form factor ratios has been studied and has been found to shift the position of the asymmetry zero about 5% towards larger values. We are now in the position to discuss the effect of both, factorizable *and* non-factorizable radiative corrections to next-to-leading order in the strong coupling constant on the location of the asymmetry-zero, and hence to complete our earlier analysis.

We define the forward-backward (FB) asymmetry (normalized to the differential decay rate $d\Gamma(B^- \rightarrow K^{*-}\ell^+\ell^-)/dq^2$) by

$$\frac{dA_{\text{FB}}}{dq^2} \equiv \frac{1}{d\Gamma/dq^2} \left(\int_0^1 d(\cos\theta) \frac{d^2\Gamma}{dq^2 d\cos\theta} - \int_{-1}^0 d(\cos\theta) \frac{d^2\Gamma}{dq^2 d\cos\theta} \right) \quad (72)$$

Our result for the FB asymmetry is shown in Figure 9 to LO and NLO accuracy. From (64) it is obvious that $dA_{\text{FB}}/dq^2 \propto \text{Re}(\mathcal{C}_{9,\perp}(q^2))$, and therefore the FB asymmetry vanishes if $\text{Re}(\mathcal{C}_{9,\perp}(q_0^2)) = 0$. At leading order this translates into the relation

$$C_9 + \text{Re}(Y(q_0^2)) = -\frac{2M_B m_b}{q_0^2} C_7^{\text{eff}} \quad , \quad (73)$$

which, as already mentioned, is free of hadronic uncertainties. This effect can also be seen in Figure 9 where the uncertainty for the prediction of the FB asymmetry gets smaller around q_0^2 . Using our default input parameters we obtain $q_0^2 = 3.4_{-0.5}^{+0.6}$ GeV² at LO where the error is by far dominated by the scale dependence. The numerical effect of NLO corrections amounts to a substantial reduction of the FB asymmetry for intermediate lepton invariant mass ($q^2 = 2 - 5$ GeV²) and a significant shift of the location of the asymmetry zero to

$$q_0^2 = 4.39_{-0.35}^{+0.38} \text{ GeV}^2 \quad (74)$$

The largest single uncertainty (about ± 0.25 GeV²) continues to be scale dependence (varying μ within $m_b/2 < \mu < 2m_b$ as usual), but also the variation of m_b , Λ_{QCD} , and $\lambda_{B,+}$ gives an effect.

Our LO result for q_0^2 differs somewhat from the value $q_0^2 = 2.88_{-0.28}^{+0.44}$ quoted in [32]. The reason for this difference is a combination of three effects: (i) slightly different values for the SM Wilson coefficients, in particular a larger value for C_9 in [32], (ii) a different treatment of the b -quark mass, (iii) the inclusion of (higher-order factorizable) form factor corrections in [32], since the full QCD form factors estimated from light-cone QCD sum rules [17] are used. The first two issues are resolved within the present next-to-leading order treatment but with respect to (iii) we note that the form factor ratios entering $\mathcal{C}_{9,\perp}$ are exactly those where there exists a discrepancy between the QCD sum rule result and the heavy quark limit [4]. The origin of this discrepancy has not been clarified, but it is conceivable that it is related to some $1/M_B$ corrections, which are implicitly included in the sum rule estimate. In order to estimate the impact of using full QCD form factors on the location of the asymmetry zero, we reabsorb the factorizable α_s corrections into the physical form factors and the $\overline{\text{MS}}$ mass. The FB asymmetry then reads (with the tensor form factors and the $\overline{\text{MS}}$ mass \hat{m}_b all renormalized at the scale μ)

$$\begin{aligned} \frac{dA_{\text{FB}}}{dq^2} = & -\frac{1}{d\Gamma/dq^2} \frac{G_F^2 |V_{ts}^* V_{tb}|^2}{128\pi^3} M_B^3 \lambda(q^2, m_{K^*}^2)^2 \left(\frac{\alpha_{\text{em}}}{4\pi} \right)^2 \frac{8q^2}{M_B^2} C_{10} A_1(q^2) V(q^2) \\ & \times \text{Re} \left[\left(C_9 + Y(q^2) + \frac{\alpha_s C_F}{4\pi} C_{\perp}^{(\text{nf},9)}(q^2) \right) \right. \\ & + \frac{\hat{m}_b}{q^2} \left((M_B + m_{K^*}) \frac{T_1(q^2)}{V(q^2)} + (M_B - m_{K^*}) \frac{T_2(q^2)}{A_1(q^2)} \right) \\ & \times \left(C_7^{\text{eff}} + \frac{\alpha_s C_F}{4\pi} C_{\perp}^{(\text{nf},7)}(q^2) \right) \\ & + \frac{\hat{m}_b}{q^2} \left((M_B + m_{K^*}) \frac{1}{V(q^2)} + (M_B - m_{K^*}) \left(1 - \frac{q^2}{M_B^2} \right) \frac{1}{A_1(q^2)} \right) \\ & \left. \times \frac{\alpha_s C_F}{4\pi} \frac{\pi^2}{N_c} \frac{f_B f_{K^*,\perp} \lambda_{B,+}^{-1}}{M_B} \int_0^1 du \Phi_{K^*,\perp}(u) T_{\perp,+}^{(\text{nf})}(u) \right] \quad (75) \end{aligned}$$

The non-factorizable contributions from $C_{\perp}^{(\text{nf})}$ in (37) are now divided into two parts,

coming with the operator structure of \mathcal{O}_7 and \mathcal{O}_9 , respectively,

$$C_F C_\perp^{(\text{nf},9)}(q^2) = - \left[\bar{C}_2 F_2^{(9)}(q^2) + 2\bar{C}_1 \left(F_1^{(9)}(q^2) + \frac{1}{6} F_2^{(9)}(q^2) \right) + C_8^{\text{eff}} F_8^{(9)}(q^2) \right], \quad (76)$$

$$C_F C_\perp^{(\text{nf},7)}(q^2) = - \left[\bar{C}_2 F_2^{(7)}(q^2) + C_8^{\text{eff}} F_8^{(7)}(q^2) \right]. \quad (77)$$

These are just the terms that also enter the inclusive decay, while the last term in (75) arises from the hard spectator-scattering and thus only appears in the exclusive decay. Using the relations $T_2 = 2ET_1/M_B$ and $A_1 = 2EM_B V/(M_B + m_{K^*})^2$, which are presumed to hold to all orders in α_s , and to leading order in $1/m_b$ [4, 12], (75) can be rearranged to contain only V and T_1/V . If furthermore the latter ratio is expanded in α_s and if some terms of order $m_{K^*}^2/M_B^2$ are neglected, we return to the next-to-leading order result that we use by default. On the basis of (75) and the form factor estimates from [17], we now obtain $q_0^2 = 3.25 \text{ GeV}^2$ at LO and $q_0^2 = 3.94 \text{ GeV}^2$ at NLO. (To obtain this result we use $m_{b,\text{PS}}$ as input and treat perturbatively the difference with \hat{m}_b .) The NLO value is slightly more than one “standard deviation” away from our default result in (74). The difference between the two values could be viewed as an estimate for an additional systematic error, but the main conclusion is that using the soft form factors or the full QCD form factors from light-cone QCD sum rules does not cause a large ambiguity in our result for q_0^2 . We therefore assume

$$q_0^2 = (4.2 \pm 0.6) \text{ GeV}^2 \quad (78)$$

to be a conservative estimate for the asymmetry zero.

The Wilson coefficients may also receive contributions from new particles in theories beyond the standard model. (Of course extensions of the standard model may introduce a larger set of operators as well.) The function $\mathcal{C}_{9,\perp}$ depends dominantly on C_9 and C_7^{eff} (see (40)). The experimental measurement of the decay rate for the inclusive decay $\bar{B} \rightarrow X_s \gamma$ already constrains $|C_7^{\text{eff}}|$ to be close to its standard model value. The forward-backward asymmetry will establish the sign of C_7^{eff} and assuming this to take its standard model value, a measurement of the FB asymmetry zero in the decay $\bar{B} \rightarrow \bar{K}^* \ell^+ \ell^-$ provides a way to determine C_9 . It is therefore instructive to consider our result as a prediction for C_9 for a given value of q_0^2 that will be measured in future experiments. In Figure 10 we show our NLO prediction for C_9 at the scale $\mu = 4.6 \text{ GeV}$ as a function of q_0^2 together with the standard model prediction (see Section 3.1). For comparison we also show the LO result and the modification arising from using (75) instead of (64). We remark that C_9 is scheme-dependent and so the plot refers to the particular renormalization scheme for \mathcal{O}_9 adopted in [6].

Figure 10 is our main phenomenological result. It illustrates that the FB asymmetry zero can be used to test the standard model and to search for extensions, since the theoretical uncertainties relevant for the determination of C_9 are under control. In this respect the systematic inclusion of NLO corrections, which is provided in this work, turns out to be essential, because it reduces the renormalization scale and scheme dependences to a large extent and corrects the leading-order result by a large amount. We emphasize that in contrast to the absolute rates for $\bar{B} \rightarrow \bar{K}^* \gamma$ and $\bar{B} \rightarrow \bar{K}^* \ell^+ \ell^-$ the dependence on the $\bar{B} \rightarrow \bar{K}^*$ form factors is sub-leading for the FB asymmetry zero. Thus the

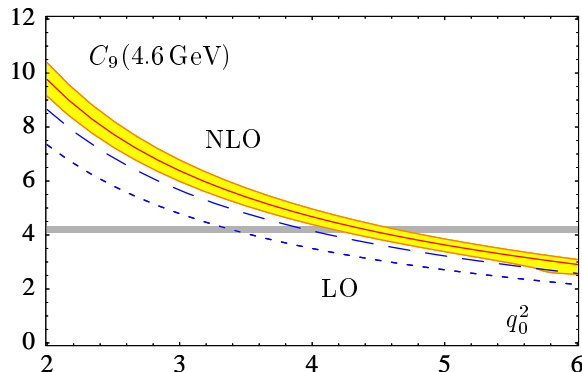


Figure 10: The Wilson coefficient $C_9(m_b)$ deduced from a measurement of the asymmetry zero q_0 at next-to-leading order including all parameter uncertainties (light band), but not including the slightly enlarged error in (78). For comparison we also show (without uncertainties) the leading order result (dashed) and the result at next-to-leading order using (75) and the full QCD form factors from [17] (long-dashed). The horizontal band is the standard model value $C_9(4.6 \text{ GeV}) = 4.21 \pm 0.12$.

current difficulty to account for the $\bar{B} \rightarrow \bar{K}^* \gamma$ branching ratio (which may suggest a smaller value of the form factor $T_1(0)$ than usually estimated from QCD sum rules as discussed above), does not necessarily cause a problem for our prediction of C_9 vs. q_0^2 . We also note that the resulting values of q_0^2 are sufficiently below the threshold for charmonium resonances (J/ψ , ψ'), so that a long-distance contribution to the function $Y(q^2)$ can safely be neglected. We therefore conclude that if the asymmetry zero is found at some $q_0^2 < 6 \text{ GeV}^2$, the short-distance coefficient $C_9(4.6 \text{ GeV})$ can be determined with a theoretical error of $\pm 10\%$. If its value turns out to be different from the standard model value 4.21 ± 0.12 by an amount Δ and if we assume that all Wilson coefficients other than $C_{9,10}$ remain unmodified at the scale M_W , then (97) below implies a new contribution of magnitude Δ to the coefficient function C_9 at the scale M_W .

6 Concluding discussion

Building on our previous work on heavy-to-light form factors [4] and on work on non-leptonic decays [2, 3], we demonstrated that also the radiative B decays $B \rightarrow V \gamma$ and $B \rightarrow V \ell^+ \ell^-$ can be computed in the heavy-quark limit. This allows us to solve the problem of non-factorizable strong interaction corrections (i.e. those corrections not related to form factors), which has so far prevented a systematic discussion of exclusive radiative decays, as compared to their inclusive analogues. The approach presented here does not circumvent the need to know the heavy-to-light form factors, but we may hope that progress in lattice QCD will give us these form factors at smaller q^2 and more reliably than at present in the longer term future.

In the present paper we have concentrated on the $b \rightarrow s$ transition. We noted that the

next-to-leading order correction yields an 80% enhancement of the $B \rightarrow K^*\gamma$ decay rate, a large part of which is related to the NLO correction that appears also in the inclusive decay [9, 10]. The enhancement is so large that the predicted decay rate disagrees with the observed decay rate unless the form factors at $q^2 = 0$ are much smaller than what they are believed to be, or unless our theoretical prediction is made unreliable by a large correction to the heavy quark limit. Perhaps the most interesting outcome of our analysis is that while the NLO correction to the lepton invariant mass spectrum in $B \rightarrow K^*\ell^+\ell^-$ is very small, there is a large correction to the predicted location of the forward-backward asymmetry zero. The particular interest in this quantity derives from the fact that all dependence of form factors arises first at next-to-leading order. This implies that (given the Wilson coefficient C_7) the Wilson coefficient C_9 can be determined from a measurement of the location of the asymmetry zero with little theoretical uncertainty. We find that this conclusion holds true in particular after including the NLO correction, which however, shifts the predicted location of the zero by 1 GeV^2 , or about 30%, with a residual uncertainty estimated to be about $(0.4 - 0.6) \text{ GeV}^2$. This implies that an accurate measurement of the asymmetry zero determines the Wilson coefficient C_9 at the scale m_b with an error of $\pm 10\%$.

The method developed here can also be applied to $b \rightarrow d$ transitions. These are particularly interesting in the search for modifications of the standard model. The better control of standard model effects after accounting for non-factorizable corrections should help increasing the sensitivity to such non-standard effects. In particular we note that the approach presented here allows us to compute isospin breaking effects, which may turn out to be a particularly nice signal of non-standard physics. A detailed discussion of $b \rightarrow d$ transitions requires, however, a more careful study of weak annihilation effects, and we plan to return to non-standard physics in the context of such a study [29].

A systematic, but rather difficult to quantify, limitation of the factorization approach is the poor control of $1/m_b$ suppressed effects. These arise from various sources and we conclude by mentioning one of them. We may ask to what extent a non-leptonic decay $B \rightarrow K^*\rho$ in which the ρ meson is assumed to convert to a photon through vector meson dominance may affect our calculation of the direct decay into $K^*\gamma^*$. More accurately, the question is to what extent the hadronic structure of the photon matters at small q^2 . It is not difficult to see that the indirect contribution is suppressed by one power of m_b in the heavy quark limit. For the sake of the argument we return to the vector dominance picture and note that there is a one-to-one correspondence between diagrams that appear in the factorization approach to non-leptonic decays [2, 3] and the diagrams computed here. For example, the naive factorization contribution to the former case corresponds to our leading order weak annihilation term; the spectator scattering contribution to non-leptonic decays corresponds to the diagram in Figure 2b with the photon attached to the internal quark loop and so on. Counting powers of m_b for all the quantities that appear in these amplitudes we find that the direct amplitude is always larger by a factor of m_b .

Acknowledgements

We would like to thank C. Greub and M. Walker for helpful discussions. While this work has been done, we became aware of related work in [28]. We thank G. Buchalla for discussing the results of this paper prior to publication.

Note added

While completing this work, the article [33] appeared, in which the next-to-leading order hard-scattering correction to $B \rightarrow \rho\gamma$ is calculated. The corresponding quantity should be obtained from the function $T_{\perp,+}^{(\text{nf})}$ in (23) in the limit $q^2 \rightarrow 0$. The small QCD penguin contributions have been neglected in [33], so that only the terms proportional to \bar{C}_2 and C_8^{eff} have to be retained for the comparison. The charm quark mass in $t_{\perp}(u, m_c)$ is set to 0 in [33], presumably because an endpoint divergence is found for $m_c \neq 0$. We note that our result does not exhibit this endpoint divergence (which would invalidate the factorization approach), but setting $m_c = 0$ for the sake of comparison, we obtain

$$T_{\perp,+}^{(\text{nf})}(u, \omega) \rightarrow -\frac{4e_d C_8^{\text{eff}}}{u} + \frac{M_B}{2m_b} \frac{4e_u \bar{C}_2}{\bar{u}}.$$

We then differ from (4.12) of [33] by a sign in the first term and a factor of -4 in the second term. We also note that [33] includes a factorizable form factor correction from [4] while retaining the full QCD form factor $T_1(0)$. This implies that the factorizable correction is included twice.

A Operator bases

We use the renormalization conventions of [6], but present our result in terms of the following linear combinations of Wilson coefficients:

$$\begin{aligned}\bar{C}_1 &= \frac{1}{2} C_1, \\ \bar{C}_2 &= C_2 - \frac{1}{6} C_1, \\ \bar{C}_3 &= C_3 - \frac{1}{6} C_4 + 16 C_5 - \frac{8}{3} C_6, \\ \bar{C}_4 &= \frac{1}{2} C_4 + 8 C_6, \\ \bar{C}_5 &= C_3 - \frac{1}{6} C_4 + 4 C_5 - \frac{2}{3} C_6, \\ \bar{C}_6 &= \frac{1}{2} C_4 + 2 C_6.\end{aligned}\tag{79}$$

These definitions hold to all orders in perturbation theory. The “barred” coefficients are related to those defined in [7] by [34]

$$\bar{C}_i = C_i^{\text{BBL}} + \frac{\alpha_s}{4\pi} T_{ij} C_j^{\text{BBL}} + O(\alpha_s^2),\tag{80}$$

where

$$T = \begin{pmatrix} \frac{7}{3} & 2 & 0 & 0 & 0 & 0 \\ 1 & -\frac{2}{3} & 0 & 0 & 0 & 0 \\ 0 & 0 & -\frac{178}{27} & -\frac{4}{9} & \frac{160}{27} & \frac{13}{9} \\ 0 & 0 & \frac{34}{9} & \frac{20}{3} & -\frac{16}{9} & -\frac{13}{3} \\ 0 & 0 & \frac{164}{27} & \frac{23}{9} & -\frac{146}{27} & -\frac{32}{9} \\ 0 & 0 & -\frac{20}{9} & -\frac{23}{3} & \frac{2}{9} & \frac{16}{3} \end{pmatrix}. \quad (81)$$

B Unexpanded form of $F_8^{(7,9)}$

Using the conventions of [10] we obtain for the 1-loop matrix element of \mathcal{O}_8 (Figure 2c together with a set of symmetric diagrams):

$$F_8^{(7)} = -\frac{32}{9} \ln \frac{\mu}{m_b} - \frac{8}{9} \frac{\hat{s}}{1-\hat{s}} \ln \hat{s} - \frac{8}{9} i\pi - \frac{4}{9} \frac{11 - 16\hat{s} + 8\hat{s}^2}{(1-\hat{s})^2} + \frac{4}{9} \frac{1}{(1-\hat{s})^3} \left[(9\hat{s} - 5\hat{s}^2 + 2\hat{s}^3) B_0(\hat{s}) - (4 + 2\hat{s}) C_0(\hat{s}) \right], \quad (82)$$

$$F_8^{(9)} = \frac{16}{9} \frac{1}{1-\hat{s}} \ln \hat{s} + \frac{8}{9} \frac{5 - 2\hat{s}}{(1-\hat{s})^2} - \frac{8}{9} \frac{4 - \hat{s}}{(1-\hat{s})^3} [(1 + \hat{s}) B_0(\hat{s}) - 2 C_0(\hat{s})], \quad (83)$$

where $\hat{s} = q^2/m_b^2$, $B_0(\hat{s}) = B_0(q^2, m_b^2)$ is given in (29), and the integral

$$C_0(\hat{s}) = \int_0^1 dx \frac{1}{x(1-\hat{s})+1} \ln \frac{x^2}{1-x(1-x)\hat{s}} \quad (84)$$

can be expressed in terms of dilogarithms.

C NNLL formulae for C_9 and $C_{1,\dots,6}$

Because the anomalous dimension of \mathcal{O}_9 begins at order α_s^0 , the Wilson coefficient C_9 is needed to next-to-next-to-leading logarithmic (NNLL) accuracy. This requires also the coefficient of the four-quark operators to this accuracy. Although not all of the necessary inputs are currently known, we present here the solution of the renormalization group equations to NNLL order.

We first restrict ourselves to the sector of four-quark operators. Define $a_s(\mu) = \alpha_s(\mu)/(4\pi)$ and $\beta(a_s) = \beta_0 a_s^2 + \dots$ with $\beta_0 = 11 - 2n_f/3$. We further define the matrix $U(\mu, M_W)$ such that

$$C(\mu) = U(\mu, M_W) C(M_W), \quad (85)$$

where $C(\mu)$ is the vector of Wilson coefficients. $U(\mu, M_W)$ satisfies

$$\frac{d}{d \ln \mu} U(\mu, M_W) = \gamma^T(\mu) U(\mu, M_W), \quad (86)$$

and the anomalous dimension matrix is expanded as

$$\gamma = \gamma^{(0)} a_s + \gamma^{(1)} a_s^2 + \dots \quad (87)$$

Let V be the matrix that diagonalizes $\gamma^{(0)T}$, so that

$$V^{-1} \gamma^{(0)T} V = \left[\gamma_i^{(0)} \right]_{\text{diag}}, \quad (88)$$

and define

$$U^{(0)}(\mu, M_W) = V \left[\left(\frac{a_s(\mu)}{a_s(M_W)} \right)^{-\gamma_i^{(0)}/(2\beta_0)} \right]_{\text{diag}} V^{-1}, \quad (89)$$

which solves (86) to leading order in $a_s(\mu)$. Then the NNLL expression for the evolution matrix $U(\mu, M_W)$ reads

$$\begin{aligned} U(\mu, M_W) &= \left(1 + a_s(\mu) J^{(1)} + a_s(\mu)^2 J^{(2)} \right) U^{(0)}(\mu, M_W) \\ &\times \left(1 - a_s(M_W) J^{(1)} - a_s(M_W)^2 \left[J^{(2)} - J^{(1)2} \right] \right), \end{aligned} \quad (90)$$

where

$$J^{(n)} = V H^{(n)} V^{-1}. \quad (91)$$

The matrices $H^{(1)}$, $H^{(2)}$ have the entries

$$H_{ij}^{(1)} = \delta_{ij} \gamma_i^{(0)} \frac{\beta_1}{2\beta_0^2} - \frac{G_{ij}^{(1)}}{2\beta_0 + \gamma_i^{(0)} - \gamma_j^{(0)}}, \quad (92)$$

$$\begin{aligned} H_{ij}^{(2)} &= \delta_{ij} \gamma_i^{(0)} \frac{\beta_2}{4\beta_0^2} + \sum_k \frac{2\beta_0 + \gamma_i^{(0)} - \gamma_k^{(0)}}{4\beta_0 + \gamma_i^{(0)} - \gamma_j^{(0)}} \left(H_{ik}^{(1)} H_{kj}^{(1)} - \frac{\beta_1}{\beta_0} H_{ij}^{(1)} \delta_{jk} \right) \\ &- \frac{G_{ij}^{(2)}}{4\beta_0 + \gamma_i^{(0)} - \gamma_j^{(0)}} \end{aligned} \quad (93)$$

and we have defined

$$G^{(n)} = V^{-1} \gamma^{(n)T} V. \quad (94)$$

The same equations can also be used to solve the renormalization group equations when the electromagnetic and chromomagnetic dipole operators are included. Then γ is an 8×8 matrix, and one needs to keep in mind that the 6×2 block in $\gamma^{(n)}$ that mixes the dipole and four-quark operators is obtained from $n + 2$ loop diagrams, while all other entries come from $n + 1$ loop diagrams. In our numerical analysis we expand $U(\mu, M_W) C(M_W)$ in powers of $a_s(\mu)$ and $a_s(M_W)$ using (90) and the expansion of the initial condition $C(M_W)$ in powers of $a_s(M_W)$ and keep only terms to the required order in both expansion parameters.

The renormalization group equation for C_9 is particularly simple and can be obtained directly by integrating the coefficients of four-quark operators. The equation reads

$$\frac{d}{d \ln \mu} C_9(\mu) = \kappa(\mu) C(\mu), \quad (95)$$

where $C(\mu)$ is the vector of Wilson coefficients of four-quark operators and

$$\kappa = \kappa^{(-1)} + \kappa^{(0)} a_s + \dots \quad (96)$$

is the 1×6 matrix that describes the mixing into \mathcal{O}_9 . The calculation of $\kappa^{(n)}$ involves $n + 2$ loop diagrams. The solution of (95) is given by

$$C_9(\mu) = C_9(M_W) + W(\mu, M_W) C(M_W), \quad (97)$$

with the 1×6 matrix

$$W(\mu, M_W) = -\frac{1}{2} \int_{a_s(M_W)}^{a_s(\mu)} da_s \frac{\kappa(a_s)}{\beta(a_s)} U(\mu, M_W) \quad (98)$$

with the evolution matrix $U(\mu, M_W)$ from the four-quark sector as defined above. The solution to NNLL accuracy is obtained by inserting $U(\mu, M_W)$ to this accuracy. We introduce the 6×6 matrices

$$D_n(\mu, M_W) = V \left[\frac{1}{n - \gamma_i^{(0)}/(2\beta_0)} \left[\left(\frac{a_s(\mu)}{a_s(M_W)} \right)^{n - \gamma_i^{(0)}/(2\beta_0)} - 1 \right] \right]_{\text{diag}} V^{-1}, \quad (99)$$

in terms of which the solution is given by

$$\begin{aligned} W(\mu, M_W) = & -\frac{\kappa^{(-1)}}{2\beta_0 a_s(M_W)} D_{-1}(\mu, M_W) \\ & -\frac{1}{2\beta_0} \left[\left(\kappa^{(0)} - \frac{\beta_1}{\beta_0} \kappa^{(-1)} + \kappa^{(-1)} J^{(1)} \right) D_0(\mu, M_W) - \kappa^{(-1)} D_{-1}(\mu, M_W) J^{(1)} \right] \\ & -\frac{a_s(M_W)}{2\beta_0} \left[\left(\kappa^{(1)} - \frac{\beta_1}{\beta_0} \kappa^{(0)} + \left(\frac{\beta_1^2}{\beta_0^2} - \frac{\beta_2}{\beta_0} \right) \kappa^{(-1)} + \left(\kappa^{(0)} - \frac{\beta_1}{\beta_0} \kappa^{(-1)} \right) J^{(1)} \right. \right. \\ & \quad \left. \left. + \kappa^{(-1)} J^{(2)} \right) D_1(\mu, M_W) - \left(\kappa^{(0)} - \frac{\beta_1}{\beta_0} \kappa^{(-1)} + \kappa^{(-1)} J^{(1)} \right) D_0(\mu, M_W) J^{(1)} \right. \\ & \quad \left. \left. - \kappa^{(-1)} D_{-1}(\mu, M_W) [J^{(2)} - J^{(1)2}] \right] \right] \quad (100) \end{aligned}$$

In our numerical analysis we expand (97) in powers of $a_s(M_W)$ and keep only terms to the required order in the expansion parameter. To NNLL we thus need $C_9(M_W)$ to order a_s and since the first term in the expansion of this quantity is of order a_s^0 , we recover from (100) the well-known result that the LL solution for C_9 is induced only by mixing and is of order $1/a_s$.

References

- [1] R. Ammar *et al.* [CLEO Collaboration], Phys. Rev. Lett. **71** (1993) 674.

- [2] M. Beneke, G. Buchalla, M. Neubert and C. T. Sachrajda, Phys. Rev. Lett. **83** (1999) 1914 [hep-ph/9905312].
- [3] M. Beneke, G. Buchalla, M. Neubert and C. T. Sachrajda, Nucl. Phys. B **591** (2000) 313 [hep-ph/0006124].
- [4] M. Beneke and T. Feldmann, Nucl. Phys. B **592** (2001) 3 [hep-ph/0008255].
- [5] J. Charles, A. Le Yaouanc, L. Oliver, O. Pene and J. C. Raynal, Phys. Rev. D **60** (1999) 014001 [hep-ph/9812358].
- [6] K. Chetyrkin, M. Misiak and M. Münz, Phys. Lett. B **400** (1997) 206 [hep-ph/9612313].
- [7] G. Buchalla, A. J. Buras and M. E. Lautenbacher, Rev. Mod. Phys. **68** (1996) 1125 [hep-ph/9512380].
- [8] H. H. Asatrian, H. M. Asatrian and D. Wyler, Phys. Lett. B **470** (1999) 223 [hep-ph/9905412].
- [9] C. Greub, T. Hurth and D. Wyler, Phys. Rev. D **54** (1996) 3350 [hep-ph/9603404].
- [10] H. H. Asatrian, H. M. Asatrian, C. Greub and M. Walker, Phys. Lett. B **507** (2001) 162 [hep-ph/0103087].
- [11] B. Grinstein, M. J. Savage and M. B. Wise, Nucl. Phys. B **319** (1989) 271.
- [12] G. Burdman and G. Hiller, Phys. Rev. D **63** (2001) 113008 [hep-ph/0011266].
- [13] B. Grinstein and D. Pirjol, Phys. Rev. D **62** (2000) 093002 [hep-ph/0002216].
- [14] C. Bobeth, M. Misiak and J. Urban, Nucl. Phys. B **574** (2000) 291 [hep-ph/9910220].
- [15] M. Beneke, Phys. Lett. B **434** (1998) 115 [hep-ph/9804241].
- [16] M. Beneke and A. Signer, Phys. Lett. B **471** (1999) 233 [hep-ph/9906475].
- [17] P. Ball and V. M. Braun, Phys. Rev. D **58** (1998) 094016 [hep-ph/9805422].
- [18] G. P. Korchemsky, D. Pirjol and T. Yan, Phys. Rev. D **61** (2000) 114510 [hep-ph/9911427].
- [19] A. G. Grozin and M. Neubert, Phys. Rev. D **55** (1997) 272 [hep-ph/9607366].
- [20] M. Wirbel, B. Stech and M. Bauer, Z. Phys. C **29** (1985) 637.
- [21] C. S. Lim, T. Morozumi and A. I. Sanda, Phys. Lett. B **218** (1989) 343.
- [22] F. Krüger and L. M. Sehgal, Phys. Lett. B **380** (1996) 199 [hep-ph/9603237].
- [23] T. E. Coan *et al.* [CLEO Collaboration], Phys. Rev. Lett. **84** (2000) 5283 [hep-ex/9912057].

- [24] V. Brigljevic [BaBar Collaboration], Talk presented at the XXXVIth Rencontres de Moriond “QCD and High Energy Interactions”, March 17-24, 2001, Les Arcs, France.
- [25] G. Taylor [Belle Collaboration], Talk presented at the XXXVIth Rencontres de Moriond “Electroweak Interactions and Unified Theories”, March 17-24, 2001, Les Arcs, France.
- [26] M. Beneke, G. Buchalla, M. Neubert and C. T. Sachrajda, [hep-ph/0104110].
- [27] A. Ali, L. T. Handoko and D. London, [hep-ph/0006175].
- [28] S. Bosch and G. Buchalla, [hep-ph/0106081].
- [29] M. Beneke, T. Feldmann and D. Seidel, in preparation.
- [30] A. Ali, T. Mannel and T. Morozumi, Phys. Lett. B **273** (1991) 505.
- [31] G. Burdman, Phys. Rev. D **57**, 4254 (1998) [hep-ph/9710550].
- [32] A. Ali, P. Ball, L. T. Handoko and G. Hiller, Phys. Rev. D **61**, 074024 (2000) [hep-ph/9910221].
- [33] A. Ali and A. Y. Parkhomenko, [hep-ph/0105302].
- [34] K. Chetyrkin, M. Misiak and M. Münz, Nucl. Phys. B **520** (1998) 279 [hep-ph/9711280].